Mon. Not. R. Astron. Soc. **000**, 1–22 (2007) Printed 19 August 2008 (MN LATEX style file v2.2)

NTT follow-up observations of star cluster candidates from the FSR catalogue

D. Froebrich[1⋆†], H. Meusinger[2], and A. Scholz[3]
[1] *Centre for Astrophysics and Planetary Science, University of Kent, Canterbury, CT2 7NH, UK*
[2] *Thüringer Landessternwarte Tautenburg, Sternwarte 5, 07778 Tautenburg, Germany*
[3] *SUPA, University of St. Andrews, Department of Physics & Astronomy, North Haugh, St. Andrews, Fife, KY16 9SS, Scotland, United Kingdom*

Received sooner; accepted later

ABSTRACT

We are conducting a large program to classify newly discovered Milky Way star cluster candidates from the list of Froebrich, Scholz & Raftery (2007b). Here we present deep NIR follow-up observations from ESO/NTT of 14 star cluster candidates. We show that the combined analysis of star density maps and colour-colour/magnitude diagrams derived from deep near-infrared imaging is a viable tool to reliably classify new stellar clusters. This allowed us to identify two young clusters with massive stars, three intermediate age open clusters, and two globular cluster candidates among our targets. The remaining seven objects are unlikely to be stellar clusters. Among them is the object FSR 1767 which has previously been identified as a globular cluster using 2MASS data by Bonatto et al. (2007). Our new analysis shows that FSR 1767 is not a star cluster. We also summarise the currently available follow-up analysis of the FSR candidates and conclude that this catalogue may contain a large number of new stellar clusters, probably dominated by old open clusters.

Key words: Galaxy: globular clusters: individual; Galaxy: open clusters, individual

1 INTRODUCTION

Star clusters are the building blocks of the stellar component of galaxies. Identifying and characterising clusters is thus a crucial step for our understanding of structure formation and mass assembly in the Milky Way. The benefits of wide-field studies of stellar clusters are twofold:

i) Open clusters are currently the most important sites of star formation and early stellar evolution. In particular, the formation of massive stars is intrinsically linked to the formation of star clusters. For example, the cluster mass is thought to correlate with the mass of the most massive star in the cluster (Weidner & Kroupa (2006)). Investigating age spread, morphology, and mass segregation in a large sample of young open clusters has the potential to put limits on models for massive star formation (see review by Beuther et al. (2007)). Furthermore, by probing the distribution of masses in a diverse sample of clusters allows us to constrain the impact of environment on the outcome of star formation and to probe the diversity and the origin of the Initial Mass Function – fundamental problems in current star formation theory (see review by Bonnell et al. (2007)).

As open clusters dissolve, the stars migrate into the field. Therefore, the study of old open clusters can shed light on the timescales for cluster disruption and the underlying physical processes such as tidal interactions with giant molecular clouds, evaporation of low-mass objects, mass loss due to stellar evolution, as well as mass segregation. The currently known sample of old open clusters is very incomplete (e.g. Bonatto & Bica (2007b)). It is hence an important task to enlarge the sample of known and well classified galactic open clusters.

ii) Cluster surveys have the potential to discover new Globular Clusters (GC), a particular interesting avenue given the outstanding importance of this type of cluster. As emphasised by Harris (1996), Milky Way GCs have proven throughout the last century to be "irreplaceable objects in an amazingly wide range of astrophysical studies". The most important issue is the continuing debate about the key processes in galaxy formation and evolution. GCs have been considered for many years to be the most valuable tracers of the oldest stellar population in our galaxy.

Recent advances point to a complex picture of the genesis of our Galaxy, driven by a mixture of processes including rapid protogalactic collapse, accretion, cannibalism, galaxy collisions, and star bursts. The rich source of historical details provided by the (inhomogeneous) Milky Way GC system is among the most promising approaches to disentangle the many processes (West et al. (2004)). A complete census of the Milky Way GC system is therefore very important. More recently, a few examples of new GC classes were detected in nearby galaxies: the so-called FF ('faint fuzzies') clusters in two lenticular galaxies (Brodie & Larsen (2002)), even more

⋆ Based on observations collected at ESO, Chile; ESO 077.B-0074(A)
† E-mail: df@star.kent.ac.uk

extended GCs in the halo of M31 (Huxor et al. (2005)), very massive GCs in NGC 5128 (Martini & Ho (2004)) and ultracompact objects (perhaps bridging the gap in parameter space to dwarf galaxies) in the Fornax cluster (Mieske et al. (2002; 2004)). There are no known analogues for such unusual GCs in our galaxy where they should have been discovered unless they are hidden by dust in the classical 'Zone of Avoidance', the least complete area for the Milky Way GC sample.

Recent studies suggest that the currently known sample of Milky Way GCs is incomplete (see Bonatto et al. (2007) or Bica et al. (2007)), particularly at the low-luminosity end (the Palomar-type GCs). The number of missing GCs close to the Galactic Plane ($|z| < 0.5$ kpc) and within 3 kpc from the Galactic Centre has been estimated to $\sim 10 \pm 3$ (Ivanov et al. (2005)).

Driven by the aforementioned science goals, we have recently carried out a systematic large-scale cluster survey based on star density maps derived from the 2MASS database (Froebrich, Scholz & Raftery (2007b), hereafter FSR). The FSR survey covers the entire Galactic Plane ($|b| < 20^\circ$) and detected a total number of 1788 potential star clusters, from which 767 have been known beforehand and 1021 are unknown cluster candidates. The contamination of those candidates has been estimated to be about 50 %, indicating that the catalogue may contain up to 500 new star clusters.

In particular, the FSR survey revealed several promising GC candidates in the Zone of Avoidance. Four of them have been discussed already in detail elsewhere (Froebrich et al (2007a), (2008); Bica et al. (2007), Bonatto et al. (2007)). Given the small number (~ 150) of known galactic GCs on the one hand and the diversity of the GC species on the other hand (see above), every new GC is of value.

In this paper, we present detailed follow-up analysis for 14 cluster candidates from the FSR survey, selected to be among the best candidates for new GCs. The paper is structured as follows. In Sect. 2 we present our new observations and the reduction of the data. The detailed analysis and results for each individual cluster, including the appearance of the cluster, the contamination with field stars and the isochrone fitting to determine the cluster properties are presented in Sect. 3. Finally in Sect. 4 we discuss and conclude our findings.

2 DATA ANALYSIS

2.1 Cluster Selection

We have selected a number of cluster candidates from the FSR list for further follow up investigation. Originally 15 cluster candidates were selected, 14 of which have been observed and the results are presented in this paper. About half of the selected candidates were possible globular clusters according to the analysis in Froebrich et al. (2007b). The remainder of the objects where selected because of their interesting appearance in the 2MASS images. Since the analysis of the cluster properties was refined after the target selection for the observations, only four of the targets are still considered to be potential globular cluster candidates in the FSR list. These are FSR 0002, 0089, 1716, and 1767. Analysis of 2MASS data for three of our targets has been published (FSR 0089 - Bonatto & Bica (2007b); FSR 1754 - Bica et al. (2008); FSR 1767 - Bonatto et al. (2007)). FSR 0089 was classified as a 1 Gyr old open cluster, FSR 1754 as an uncertain case with two apparent main sequences, and FSR 1767 as a nearby Palomar type globular cluster. Another selected cluster candidate (FSR 1570 or Teutsch 143a) has been published by Pasquali et al. (2006) just before the final version of the FSR list was compiled, and is hence not in the FSR list. The cluster is very young (slightly older than 4 Myr) and contains the luminous blue variable star WRA 751. The remaining cluster candidates (FSR 0088, 0094, 1527, 1530, 1659, 1712, 1716) are investigated here for the first time in detail. Our data for FSR 1735 has already been published in Froebrich et al. (2007a). The object is most likely a globular cluster in the inner Milky Way. For completeness reasons we have added a short analysis of FSR 1735 in this paper as well.

2.2 Data

Observations have been performed in service mode using SofI at the NTT for the project ESO 077.B-0074(A). We observed each cluster candidate in J, H, and K with a pixel scale of 0.288". An eight point mosaic in the cluster candidate area was observed to cover a large enough control field in the vicinity. The candidate area was observed at the beginning and end of each mosaic, ensuring twice the per pixel integration time in the cluster candidate area. The per pixel integration time in each filter was 225 s. In general the observing conditions were clear or thin cirrus was present. In a few cases the cirrus was more thick and hence the per pixel integration time was doubled. Only for object FSR 0002 variable conditions occurred during the observations in the K band (see Sect. 3.1). The mosaics cover in total an area of about 11.7'x11.7', with the corners and the centre missing.

Standard NIR data reduction procedures were followed when creating the mosaics. Sky flats were used for flat-fielding and the xdimsum task in IRAF[1] was used for sky-subtraction and mosaicing. The average seeing FWHM in the final co-added JHK frames is between 2.5 and 3.0 pixels, corresponding to 0.7" to 0.85". This results in many regions in a severe crowding due to the high star density. Therefore, the completeness limit of the photometry is highly variable from cluster candidate to cluster candidate. The completeness limits and photometric uncertainties for each cluster candidate will be shown and discussed individually in Sect.3.

2.3 Photometry

For source detection and photometry we used the SExtractor software (Bertin & Arnouts (1996)). Due to the high star density in most fields, the limiting factor for the photometry is the confusion limit. Calibration of the images was performed using the wealth of 2MASS sources available in each field. The *rms* scatter occurring when comparing the 2MASS photometry with our measurements is rather large, in the order of 0.1 mag. This is mostly caused by our much better spatial resolution and the high star density in the images. Hence, our photometric uncertainties are also at least 0.1 mag.

Furthermore, bright stars in the images are saturated and hence their photometry is unreliable. The saturation starts for stars with a brightness between 10 and 11 mag, depending on the weather conditions and/or the seeing. At brighter magnitudes we therefore apply a separate fit of the 2MASS colours to our measured brightnesses for calibration. Still, the magnitudes become increasingly unreliable for brighter stars.

[1] IRAF is distributed by the National Optical Astronomy Observatories, which are operated by the Association of Universities for Research in Astronomy, Inc., under cooperative agreement with the National Science Foundation.

2.4 Star Density Maps

To assess the amount of stellar overdensity in the areas of the cluster candidates we created for each of the observed mosaics a star density map (SDM). For this we have used only the stars in the field with reliable photometry (quality flag of less than 4 from the SExtractor software) in all three bands. The SDM maps have a pixel size of 30" and the pixel values indicate the star density. It is determined by measuring the distance to the 50th nearest neighboring star and converting this to the star density. The combination of pixelsize and 50th nearest neighbour was chosen because of the typical star densities (10..20 stars/arcmin^2 with reliable photometry) in our images and the sizes of the cluster candidates. A typical cluster candidate should show up as a stellar overdensity in the SDMs with an extend of up to 3x3 pixels, corresponding to a radius of about 45".

The SDMs presented here show the star density in gray-scale. White corresponds to the lowest density and dark to the highest. Areas that are not covered by the mosaic or where the distance to the 50th nearest neighbour is above a set threshold are shown in black. The scaling of the pixel values from black to white is linear but different in each of the maps for the individual cluster candidates. This has been done to enhance as much as possible the contrast between the cluster candidate and control area. Since we are only interested in the relative change of the star density within an image, we will not note the maximum and minimum values for each image.

2.5 Relative Extinction Maps

Based on the SDMs, we have also created relative extinction maps (REM) for each of the mosaics. We used the same pixel size for these maps as in the SDMs. The relative extinction value is determined using the 50 nearest stars to the centre of each pixel. Two maps of the median J−H and H−K colour excess of these stars with respect to the field without cluster stars are determined. This colour excess is converted into optical extinction and both maps are averaged to obtain the final REM (see e.g. Froebrich et al. (2007c) for the conversion factors).

The presentation of the extinction values is done in gray-scale, with high extinction values in white and low extinction in black. Again, areas that are not covered by the mosaic, or were the distance to the 50th nearest neighbour is above a certain threshold, are shown in black. The scaling of extinction values is linear and, as for the SDMs, different in each of the maps to enhance as much as possible the contrast in each case. Since we are only interested in the relative extinction values within an image, we will not note the maximum and minimum values in each case.

Together, the SDMs and REMs are used during the analysis of the cluster candidates to decide which area of the mosaic is to be chosen as control field.

2.6 Decontamination of Foreground and Background Stars

The cluster candidates observed in this project are all situated close to the Galactic Plane and/or the Galactic Centre. Hence, to analyse the potential clusters we need to decontaminate the cluster field from foreground and background stars. We used the technique described in Bonatto & Bica (2007a). It counts the stars per unit area in cells of J-band magnitude and J−H and J−K colour in the cluster and the control field. Stars are then randomly removed from the cluster field according to the difference in the stellar densities in these cells. The combination of J-band magnitude and J−H and J−K colour is the optimum choice to decontaminate cluster main sequences in crowded fields (Bonatto & Bica (2007a)). The size of the cells was varied depending on the number of stars in the field. Typical values for the cell sizes are ΔJ = 0.5 mag, Δ(J−H) = 0.2 mag, and Δ(J−K) = 0.2 mag.

The correct choice of control field is obviously important for an as accurate as possible decontamination. For each cluster candidate we carefully examined the SDMs, REMs, and colour images created for each field. Control field regions were chosen so that they: i) are as close as possible to the cluster; ii) are as large as possible; iii) have no apparently higher or lower extinction values than regions close to the cluster candidate. This ensures that the control field has a foreground and background population of stars which is as similar to the cluster field as possible and contains a large enough number of stars for a sufficiently accurate statistics.

In regions where the choice of control field was difficult due to variable extinction, we compared the decontamination procedure using different control fields to ensure our choice does not influence the decontamination. In the detailed analysis of our cluster candidates in Sect. 3, we indicate the choice and reasons for the control field selection in each case. We also repeated the random decontamination process several times for each particular control field, to ensure that remaining features are real and not just due to the random nature of the process.

2.7 Colour Magnitude Diagrams

To analyse our cluster candidates in detail, we used the decontaminated J−K vs. K colour magnitude diagrams (CMD). The plotted datapoints remained in the area of the cluster after one particular realisation of the decontamination process. The solid red line in the diagrams indicates the completeness limit of the photometry. It is calculated as the peak in the luminosity function of the stars in the cluster area in each band. The completeness limit changes significantly depending on the crowding in the field and the observing conditions (as indicated above in Sect. 2.2). In some diagrams we plot two completeness limits. In these cases the upper one corresponds to the 2MASS limit in that area, the lower one represents our new data. This shows the improvement of our data compared to 2MASS and helps comparing our analysis to already published work on some of the cluster candidates. The solid black line is the best fitting isochrone to the cluster candidate. Isochrones are taken from Girardi et al. (2002).

2.8 Colour Colour Diagrams

As a second tool to analyse the cluster candidates we use decontaminated H−K vs J−H colour colour diagrams (CCD). They show the same stars (in the same colouring and symbols) as the CMDs. Overplotted are the best fitting isochrone (solid black) as well as the same isochrone without extinction (dashed black) to indicate where un-reddened main sequence and giant stars are located. The reddening path for stars is also shown, enclosed by the two straight solid black lines. The slope of the reddening path is determined using $A_\lambda \propto \lambda^\beta$ and the effective wavelength of the 2MASS filters[2], the system our brightnesses are calibrated in. If not mentioned otherwise, we use a standard value of β = 1.6.

[2] $\lambda_J = 1.235\mu$m, $\lambda_H = 1.662\mu$m, $\lambda_K = 2.159\mu$m from http://www.ipac.caltech.edu/2mass/releases/allsky/doc/explsup.html

2.9 Isochrone Fitting

To confirm the nature of the cluster candidates as real star clusters, and if so, to determine their main parameters, such as distance, age, reddening, and metallicity we use model isochrones from Girardi et al. (2002). They are overplotted into the CMDs and CCDs of the individual decontaminated cluster fields. We varied the isochrone parameters (age, metallicity) as well as the 'environmental' parameters (distance, reddening, β) until a simultaneous fit of both diagrams was found. Parameters of the best 'by-eye' fit are then taken as the cluster properties. In some cases a range of parameters can lead to a satisfying fit, and hence the cluster parameters cannot be determined accurately. These uncertainties are discussed separately for the individual objects.

2.10 Radial Star Density Profiles

For all objects that we classified as stellar cluster, we determined radial star density profiles (RDP) in order to determine their size. We used the decontaminated photometry to determine the RDPs, because this will limit statistical noise from foreground and background stars, which is significant in most cases due to the position of the clusters near the Galactic Plane. To determine the radius of the cluster, we need to obtain the RDP out to a large enough radius. Hence the decontamination has to be done for a large field around the cluster centre. In contrast, the decontamination used for the classification of the cluster candidate via CMDs and CCDs only used the central part of the candidate, to minimise the number of remaining foreground and background stars. The determined RDPs are fit using a King like profile of the form $\sigma(r) = \sigma_b + \sigma_0/(1 + (r/r_c)^2)$, where σ_b is the density of foreground and background stars remaining after the decontamination of the large field, σ_0 the central star density of the cluster, and r_c the core radius. See Sect. 4 for a discussion of the uncertainties in the determined parameters.

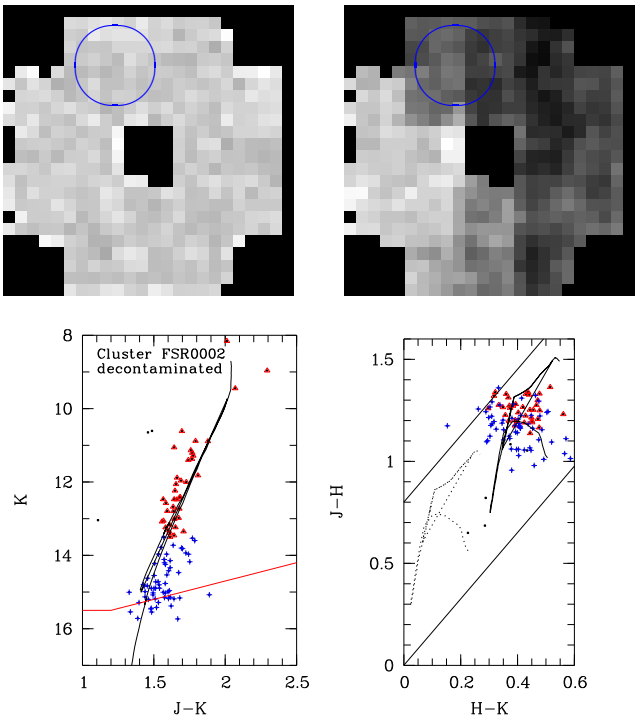

Figure 1. Top Left: SDM in the area of FSR 0002, obtained for all stars with reliable photometry in all three bands. Bright colours correspond to low star density and dark colours to high star density. The image size is 12'x12'. The circle indicates the cluster area. **Top Right:** Same scale image of the REM of the area around the cluster candidate FSR 0002 obtained from colour excess calculations. **Bottom Left:** One realisation of the decontaminated CMD. The black solid line indicates the best fitting isochrone (log(age) = 9.7, for other parameters see text) and the red line shows the completeness limit of the data. **Bottom Right:** Decontaminated CCD for FSR 0002. The best fitting isochrone is shown as solid line and its unreddened position as dashed line. The reddening path is indicated by the two straight solid lines. the colouring of the symbols is the same as in the CMD.

3 RESULTS

In the following section we will discuss in detail our results for each of the cluster candidates using the above described SDMs, REMs, CMDs, and CCDs. Together with the isochrone fitting and additional information, the plots will be used to classify the objects as a star cluster or not, and to determine its parameters. A summary of the main classification results and the parameters can be found in Table 1.

3.1 FSR 0002

The visual inspection of the cluster candidate image gives the impression of a homogeneous field of stars. This is confirmed by the SDM (top left panel in Fig. 1), which shows only small variations in the star density. The REM, however, shows large systematic differences in the colours of the stars from one side of the mosaic to the other. These differences show indications of the positions of the individual frames in the mosaic. It turns out that in this case some of the images in the K-band mosaic have been taken during cloudy conditions. Since the entire mosaic is calibrated against 2MASS sources in the field, the colours of all stars observed under cloudy conditions are systematically wrong. The calibration of the photometry with 2MASS was done using only stars in the western half of the mosaic to ensure an accurate calibration for the largest part of the field.

Given the problems with the K-band data, we have selected a control field in the western part of the mosaic. The decontamination leaves a number of stars, which in principle could be fit as a RGB/AGB of a cluster of stars. Depending on the exact position of the control field, however, a highly variable number of stars remains. There are about 1000 stars in the cluster region and depending on the choice of the control field, between 25 and 140 remain - a very small and variable fraction. Moreover, the CMDs of the cluster and any control field are extremely similar and resemble a RGB/AGB of a cluster as well.

In Fig. 1 we show one realisation of the decontamination in the CMD and CCD. Stars are represented by two different symbols/colours to facilitate the identification of groups of stars in both diagrams (i.e. distinguish between bright and faint main sequence/giant stars in the CCD). The overplotted isochrone has the parameters: Z = 0.019, log(age) = 9.7, d = 15 kpc, A_K = 0.65 mag. The only possibility to fit both diagrams simultaneously is to use a high metallicity and old age. Lower metallicity isochrones require a higher extinction to fit the CMD and hence the CCD will not be fit, except assuming very unreasonable dust properties with β much less than 1.6. Given our data analysis discussed above, we conclude

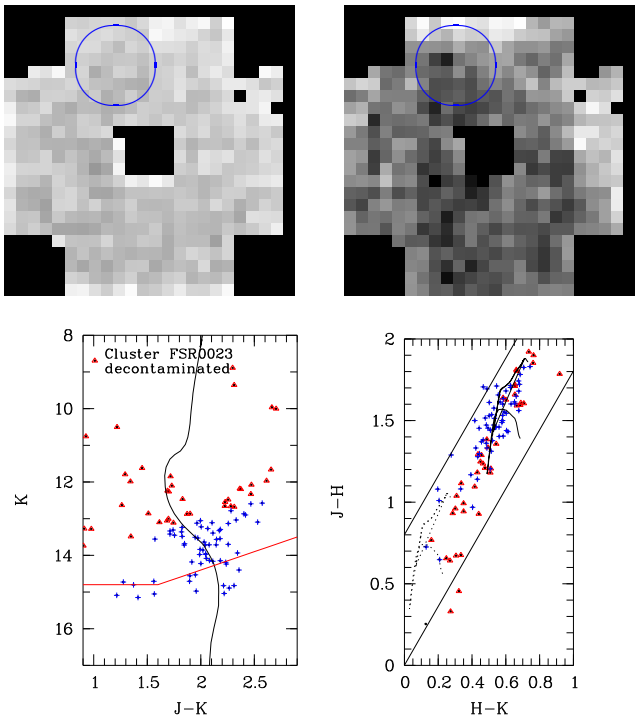

Figure 2. As Fig. 1 but for the cluster candidate FSR 0023. The plotted isochrone has log(age) = 10. See text for other parameters. Clearly no isochrone can fit all the data.

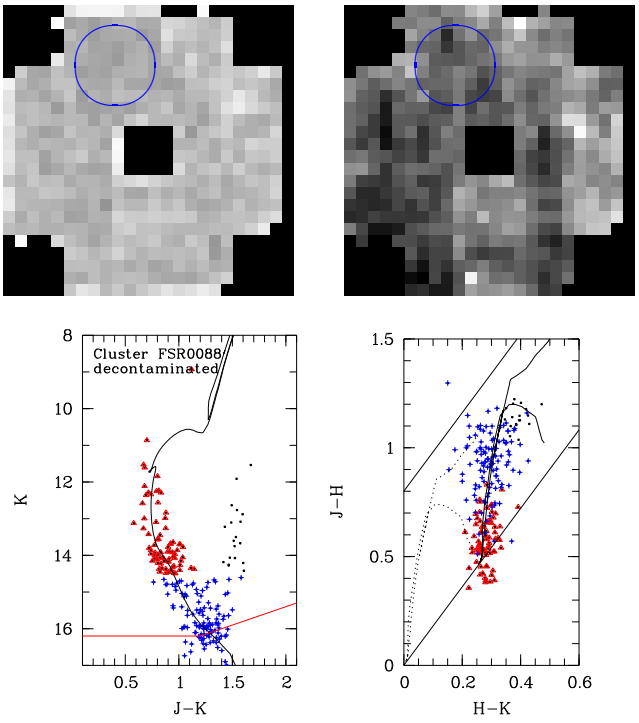

Figure 3. As Fig. 1 but for the cluster candidate FSR 0088. The plotted isochrone has log(age) = 8.7. See text for other parameters.

that it is highly unlikely that the cluster candidate FSR 0002 is a star cluster.

3.2 FSR 0023

The image of the region around the cluster candidate FSR 0023 shows no apparent cluster, as well as no significant changes of the star density. This is confirmed by the SDM. Only a slight underdensity towards the northern and western edges of the mosaic is seen. Similarly, the REM shows higher extinction values in the same regions. The lower star density and higher extinction hint that these areas are influenced by a cloud of gas and dust. Nevertheless, these regions cover only a small fraction of the entire mosaic, and we have therefore chosen as control field the entire area outside the cluster field. Choosing a smaller control field outside the cloud area in the east or south of the mosaic does not change the results.

Only a small fraction of about 10 % of the stars remain after the decontamination procedure. In the CCD and CMD it is not possible to reliably fit the remaining objects by a single isochrone with plausible parameters. In Fig. 2 we show one realisation of the decontamination with an isochrone overplotted. The parameters of the isochrone are: Z = 0.019, log(age) = 10, d = 450 pc, A_K = 0.9 mag. Again, as for FSR 0002 one needs a high metallicity old isochrone to fit the data. Given these implausible parameters, the bad agreement of any isochrone with the data, and the small number of stars remaining after the decontamination, we conclude that FSR 0023 is not a star cluster.

3.3 FSR 0088

The image of FSR 0088 shows nothing that looks like a cluster of stars. There seems to be a very slight overdensity of stars in the region around the cluster candidate, which is tentatively seen in the SDM (see Fig. 3). The REM of the entire field also shows no significant systematic differences. There are fluctuation in the map with a standard deviation of about 0.6 mag of optical extinction. These are, however, distributed in the entire mosaic and we thus use the entire area outside the cluster as the control field.

There is a large number of stars remaining after the decontamination procedure (about 25 % of the stars in the region around the cluster candidate). They are aligned along a main sequence in the CMD and the CCD. The brighter objects are located near the bottom edge of the reddening path in the CCD, indicating that those objects are stars of spectral type A. There are no or only individual giant branch stars remaining after the decontamination. Hence, there is no possibility to deduce the metallicity. The position of the cluster inside the solar circle and its apparent young/intermediate age, however, justifies the assumption of at least solar metallicity. Assuming slightly higher or lower metallicities does not change any of the following results.

We have fit an isochrone to the stars (see Fig. 3), using the upper end of the main sequence and its shape in the CMD to constrain the cluster parameters. Furthermore, the distribution of the stars in the CCD was used to determine the dust properties. We find that the best fit can be achieved with $\beta = 1.6$, an age of 500 Myr, a K-band extinction of 0.5 mag, and a distance of 2.0 kpc. The uncertainty for the age is about 60 %. The distance can be estimated within 300 pc, and the reddening within 0.05 mag K-band extinction. Outside these ranges the isochrones will clearly not fit the CMD and CCD simultaneously. The age of 0.5 Gyr means, that stars with masses of about 2.7 solar masses have just left the main sequence. These are stars of spectral type A-F, in agreement with the low J−H colours seen of those objects in the CCD.

The fact that we see no clear cluster in the image, nor a significant star density enhancement in the nearest neighbour map, could

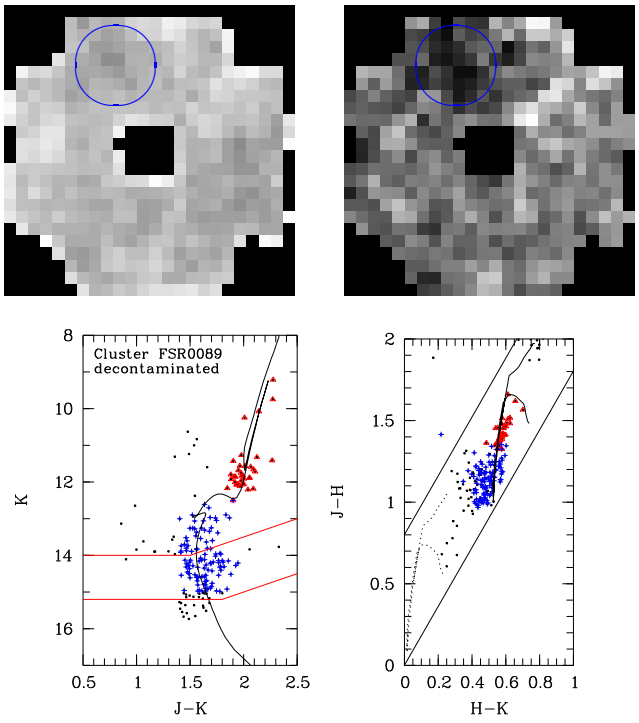

Figure 4. As Fig. 1 but for the cluster candidate FSR 0088. The plotted isochrone has log(age) = 9. See text for other parameters. The upper completeness limit in the CMD indicates the 2MASS limit.

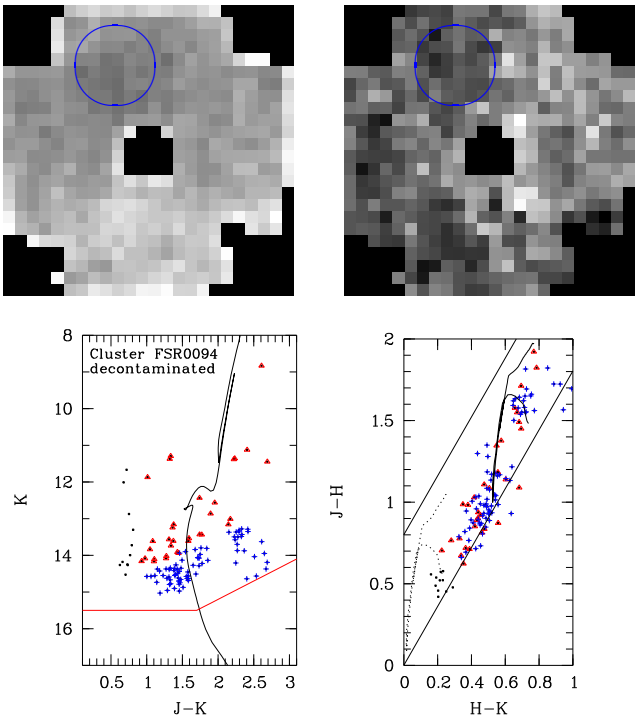

Figure 5. As Fig. 1 but for the cluster candidate FSR 0094. The plotted isochrone has log(age) = 9. See text for other parameters. Clearly no isochrone can fit all the data.

be due to the fact that we see a cluster in the process of dissolving into the field star population, which is certainly in agreement with the determined age. The RDP is very noisy and strongly depends on which realisation of the decontamination is used (see Fig. B1 for one example). It is hence not possible to measure the cluster size accurately enough.

3.4 FSR 0089

The image of the cluster candidate shows a slight overdensity of stars, especially the number of brighter stars seems to be slightly higher. This is confirmed in the SDM (see Fig. 4), which shows a higher concentration of stars in the cluster area. The REM of the mosaic shows a dip in the extinction at the position of the cluster. The A_V values in the cluster candidate area are about 2 mag lower than in the surrounding field. This either means that the stars in the cluster area are on average closer to Earth and hence bluer, the increased number of stars is caused by lower extinction at the position of the cluster candidates, or the cluster stars are intrinsically bluer than the surrounding field stars.

The 2MASS photometry of this object has been investigated in Bonatto & Bica (2007b). They classified it as a stellar cluster with an age of 1 Gyr, a distance of 2.2 kpc, and a reddening corresponding to $A_V = 9.1$ mag. The data presented here for the object is of much better spatial resolution than the 2MASS photometry, and about 1 mag deeper (see e.g. the difference in the completeness limits shown in Fig. 4). If the interpretation of Bonatto & Bica (2007b) is correct, an isochrone with their parameters should fit the new data as well.

In the decontaminated CMD of our data we have two groups of stars (about 30 % of the stars in the cluster area remain). One can be identified as giant stars and the other one as main sequence objects in a star cluster. We have overplotted our and the 2MASS observational limits in Fig. 4 to show the differences in the data. We have overplotted in the CMD an isochrone corresponding to the Bonatto & Bica (2007b) parameters. As can be seen the deeper data still agrees with the parameters found using the 2MASS photometry. We detect more of the main sequence stars, which are too faint for 2MASS. Our best fit to both, the CMD and CCD requires Z = 0.019, $\beta = 1.6$, log(age) = 9, d = 2.2 kpc, and $A_K = 1.0$ mag. Due to the presence of main sequence and giant stars we can estimate the age within 30 %. The distance is accurate within 300 pc and the reddening within 0.05 mag K-band extinction. Similar to FSR 0088, the RDP is noisy and variable. Hence no radius can be determined. Note that Bonatto & Bica (2007b) find a core radius of about 0.4 pc for this object.

There is, however, a minor detail in the data that the isochrone cannot fit: In the CCD the scatter in colours of the main sequence stars seems to point towards smaller colours, while the scatter in colour of the red giants points towards larger colours. A similar behavior, fainter stars in a cluster candidate seem to show lower extinction than brighter stars in the same candidate, can also be seen in some other examples (see below: FSR 1712, 1735). As a possible reason we have identified the calibration of our photometry with 2MASS data. Additionally to the large scatter of about 0.1 mag of the residuals in the calibration, there are some cases with even larger discrepancies for fainter magnitudes. In the case of FSR 0089, about 1/3 of the stars fainter than 12 mag in the K-band seem to be shifted by about 0.05 mag towards fainter magnitudes compared to 2MASS. This will not influence the decontamination procedure, since the colour-magnitude cells are chosen much larger than this, but it will show up in the CCDs.

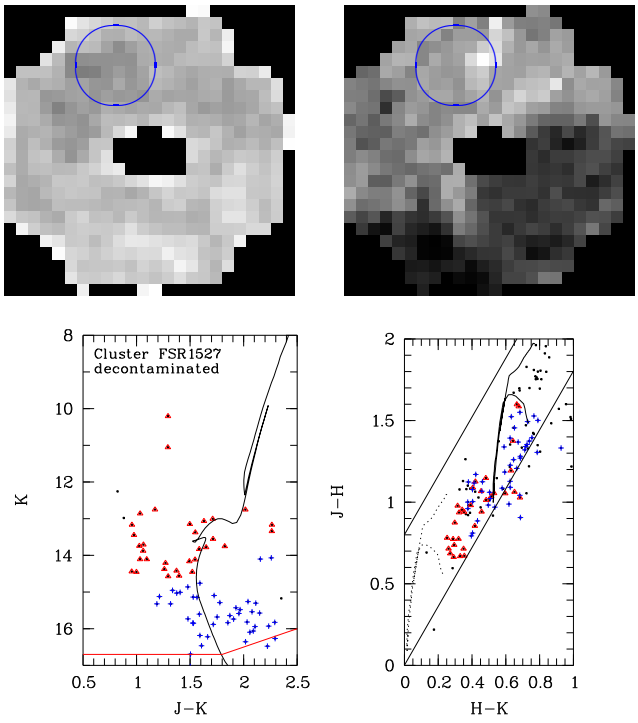

Figure 6. As Fig. 1 but for the cluster candidate FSR 1527. The plotted isochrone has log(age) = 9. See text for other parameters. Clearly no isochrone can fit all the data.

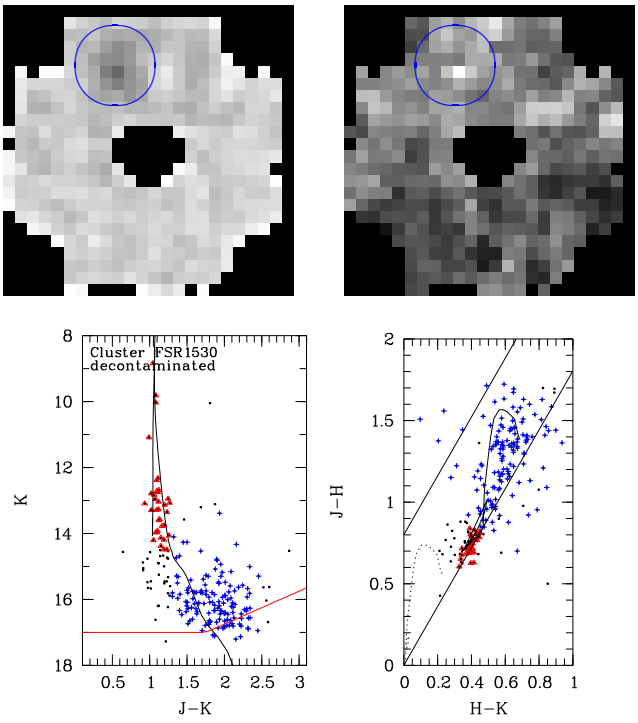

Figure 7. As Fig. 1 but for the cluster candidate FSR 1530. The plotted isochrone has log(age) = 6.6. See text for other parameters.

3.5 FSR 0094

The image of FSR 0094 seems to show a clear indication of an enhanced star density in the area of the cluster candidate. This is also apparent in the SDM (see Fig. 5). The REM shows that the western and southern part of the mosaic suffer from an increased amount of extinction compared to the area of the cluster. We have thus chosen the eastern part of the mosaic as the control area.

The stars remaining (up to 20 %) after the decontamination in the CMD and CCD clearly follow a distribution that cannot be fit by a single isochrone. Rather a range of extinction values and distances is needed. Hence, we conclude that FSR 0094 is not a cluster of stars. The isochrone in Fig. 5 is just plotted to clarify our argument that it cannot fit the data, and has the following parameters: Z = 0.019, β = 1.6, log(age) = 9, d = 2.0 kpc, and A_K = 1.0 mag.

3.6 FSR 1527

There is an indication of a cluster in the image of this region, which seems to come from a slightly larger number of brighter stars. The SDM also shows an increase in the stellar density at the position of the cluster candidate. In the REM we can identify that the southern and western side of the mosaic are subject to a lower amount of extinction than the rest of the field (see Fig. 6). We therefore choose the north-eastern part (outside the cluster candidate area) of the mosaic as control field.

The remaining stars after the decontamination (about 25 %) could to some extend be explained by an isochrone in the CMD. However, the scatter of the stars along the reddening path in the CCD is inconsistent with this proposal, i.e. with a constant reddening for all cluster stars. We conclude, that FSR 1527 is not a cluster. The isochrone in Fig. 6 is plotted to clarify our argument that it cannot fit the data, and has the following parameters: Z = 0.019, β = 1.6, log(age) = 9, d = 3.0 kpc, and A_K = 1.0 mag.

3.7 FSR 1530

The image of the cluster candidate area shows a clear enhancement of the density of stars, centred on a very bright object. This is confirmed by the SDM which has a clear indication of an overdensity of stars at the cluster candidate position. The REM shows that the southern half of the field is slightly less influenced by extinction. Therefore, we positioned the control field just west of the cluster candidate area. Furthermore, at the position of the cluster, the median colour of the stars is much redder than in the field, indicating a population of young stars, i.e. the presence of a young cluster.

The stars remaining after the decontamination (about 50 %) can be fit with an isochrone of a young cluster (see Fig. 7). The upper main sequence stars form a very compact group in the CCD with colours lying on the bottom of the reddening path, indicating spectral types earlier than A0. The other stars can be interpreted as lower mass, (pre-main sequence) objects. The best isochrone fit can be achieved using solar metallicity, an age of 4 Myr, a distance of 2.5 kpc, and A_K = 0.9 mag. It is not fully possible to fit the lower mass main sequence stars in the CCD perfectly using this isochrone. The reason might be that a lower age is required, but Girardi et al. (2002) do not provide isochrones for younger populations. As the age is small and possibly an upper limit, the determined distance is also rather uncertain. A range from 2.0 to 3.5 kpc would fit the data. The K-band extinction is uncertain by 0.05 mag. The RDP is slightly hampered by the presence of the bright star in the cluster centre. However, the profile (Fig. B3) shows a small concentrated cluster with a core radius of about 0.15 pc.

We have remeasured the central coordinates of the cluster in

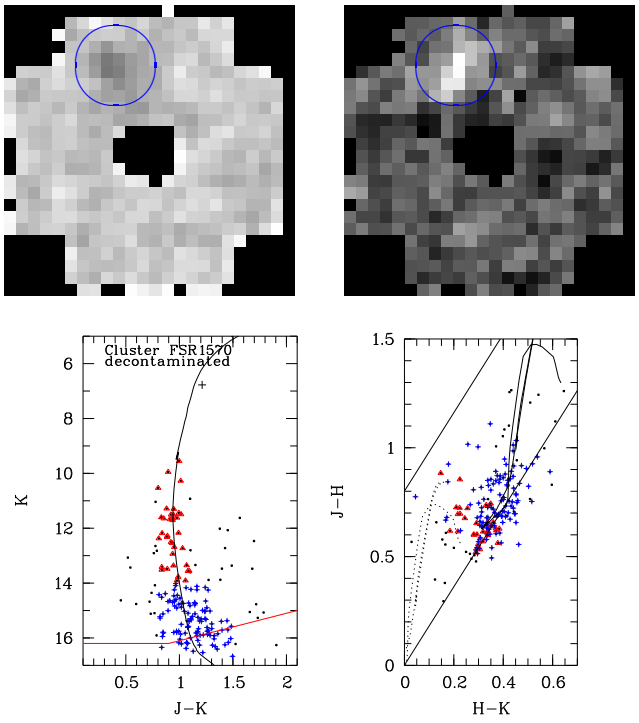

Figure 8. As Fig. 1 but for the cluster candidate FSR 1570. The plotted isochrone has log(age) = 6.9. See text for other parameters. The + in the CMD indicates the WRA 751 as measured by 2MASS.

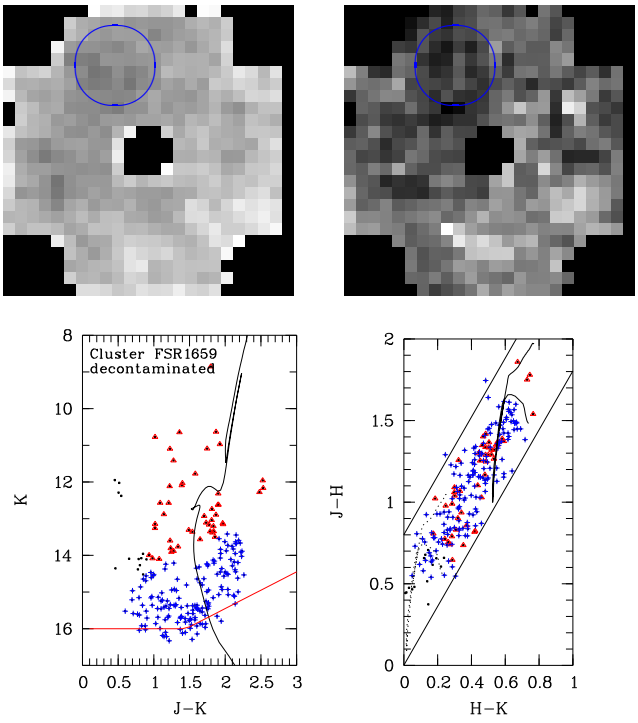

Figure 9. As Fig. 1 but for the cluster candidate FSR 1659. The plotted isochrone has log(age) = 9. See text for other parameters. Clearly no isochrone can fit all the data.

our deeper images. The central coordinates are RA = 10:08:58.3, DEC = -57:17:11 (J2000), about half an arcminute away from the values given in Froebrich et al. (2007b). The brightest star in the cluster area, [M81] I-296, projected close to the central coordinates is identified as an H_α emission line star. Its 2MASS colours and brightness are K = 7.31 mag and J−K = 1.22 mag, possibly making it a high mass cluster member.

3.8 FSR 1570

The image shows a clear concentrated cluster of stars around a very bright star. This is also evident in the SDM. The REM shows that the colours of the stars in the cluster are much redder than in the surrounding field. This indicates a young cluster. The surrounding field shows no significant fluctuations (less than 0.35 mag A_V) in the stellar colours, hence the entire area outside the cluster is used as a control field.

The cluster is known as Teutsch 143a and has been investigated with optical photometry by Pasquali et al. (2006), who identified it as the birth cluster of the galactic luminous blue variable WRA 751. The authors determine a distance of 6 kpc, an extinction of A_V = 6.1 mag, and an age of above 4 Myr.

After the decontamination about 40 % of the stars remain in the cluster field. Using β = 1.6 and an extinction of A_K = 0.8 mag, we can fit the remaining stars with an 8 Myr isochrone at a distance of 6 kpc (see Fig. 8; in the CMD we have marked with a + the position of WRA 751 obtained from 2MASS photometry since the star is saturated in our images). The bright main sequence stars are all located at the bottom of the reddening path, and are thus of spectral type earlier than A0, in agreement with Pasquali et al. (2006) who identified 24 stars with spectral types earlier than B3 in the cluster region. As the cluster is very young, the age estimate from the Girardi et al. (2002) isochrones is uncertain by a factor of two. The distance can be constrained within 1 kpc, and the K-band extinction within 0.05 mag. We have measured a core radius of about 0.35 pc for the cluster using the RDP in Fig. B4. However, the profile is influenced by the presence of WRA 751 near the centre, preventing the detection of stars nearby.

3.9 FSR 1659

The impression from the image of FSR 1659 is that there is an overdensity of stars at the position of the cluster candidate. This is confirmed in the SDM. However, as can be seen from the REM of the mosaic, the western and southern part of the area are influenced by increased amounts of extinction. Hence, the overdensity might just be caused by this effect. Therefore we have chosen the eastern part of the mosaic as the control field.

After the decontamination about 30 % of the stars remain in the cluster candidate area. However, their distribution in the CMD and CCD (see Fig. 9) cannot be fit by a single isochrone. The isochrone in Fig. 9 is plotted to clarify this argument and has the following parameters: Z = 0.019, β = 1.6, log(age) = 9, d = 2.0 kpc, and A_K = 1.0 mag. We conclude that FSR 1659 is not a star cluster.

3.10 FSR 1712

The image of FSR 1712 shows clearly a concentrated cluster of stars. This is confirmed in the SDM. The REM (see Fig. 10) of the region shows that the south-western part of the mosaic suffers from an increased value of extinction. The rest of the field shows no significant fluctuations. We have chosen the western part of the mosaic as the control area.

The decontamination procedure leaves about 40 % of the stars.

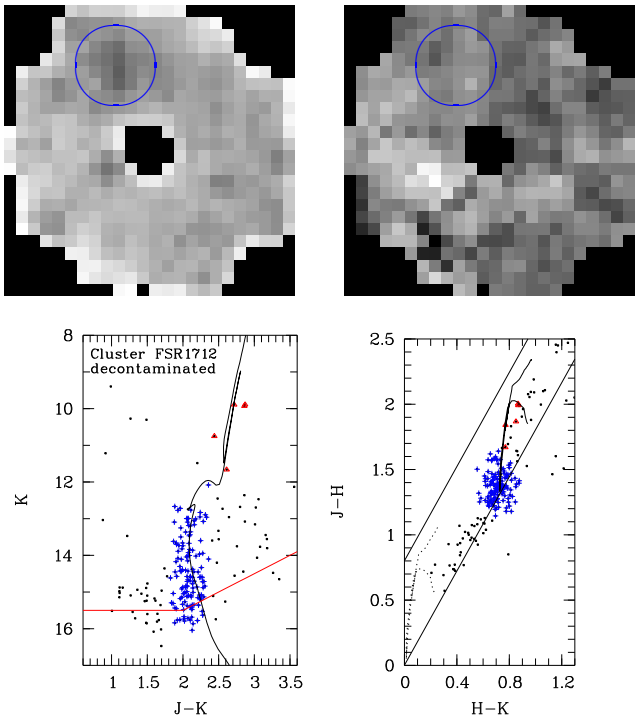

Figure 10. As Fig. 1 but for the cluster candidate FSR 1712. The plotted isochrone has log(age) = 8.9. See text for other parameters.

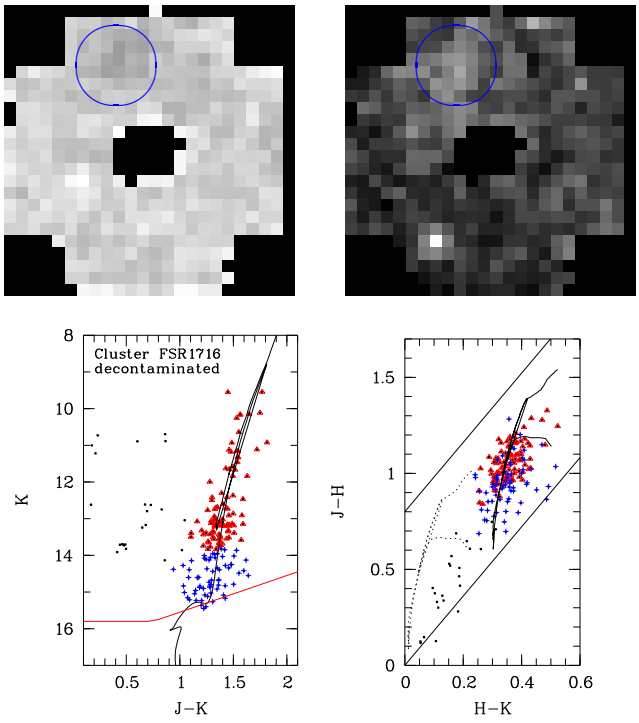

Figure 11. As Fig. 1 but for the cluster candidate FSR 1716. The plotted isochrone has log(age) = 9.3. See text for other parameters.

They can be fit by a main sequence in the CMD (see Fig. 10). The brighter stars lie close to the bottom of the reddening path, hence should be stars of spectral type A of F. Since this implies a relatively recent formation and there are no or very few red giants to determine the metallicity otherwise, we use solar metallicity isochrones.

We can fit the main sequence in the CMD and CCD using $\beta = 1.6$, an age of 0.8 Gyr, a distance of 1.8 kpc, and an extinction of A_K =1.4 mag towards the cluster. There seem to be no or only a very small number of possible red giants in the cluster. Like for FSR 0088, they seem to be shifted towards slightly redder colours in the CCD. The reason in this case might be that these few objects are actually not related to the cluster and are background red giants. This small number of giants also influences the accuracy of the age estimate, which is not better than a factor of two. The distance is accurate within 300 pc and the K-band extinction within 0.1 mag. A core radius of 0.2 pc is found for the cluster (Fig. B5), confirming the concentrated appearance in the picture.

We have remeasured the central coordinates of the cluster in our deeper images. The central coordinates are RA = 15:54:46.3, DEC = -52:31:47 (J2000), about one and a half arcminute south of the values given in Froebrich et al. (2007b). There are two ROSAT sources about 4' north and south-east of the cluster. It is not known if they are related to the cluster, but there are in total only 3 ROSAT sources within half a degree around the cluster coordinates.

3.11 FSR 1716

The image of this object shows a clear overdensity of stars, which is also confirmed in the SDM. The REM shows no significant A_V fluctuation across the field, except in the cluster candidate region, where the average colour of the stars seems to be redder than in the surrounding field (the high extinction peak in the south-east is caused by a very bright star). The redder colour of stars in this area should be intrinsic to the stars, since it comes along with an increased star density, contradicting a locally enhanced extinction due to a small cloud, which would decrease the star density. We hence use the entire field except the cluster candidate region as control area.

After the decontamination about 30 % of the stars remain. Their CMD can be interpreted as a well populated giant branch (see Fig. 11). There are two peaks in the K-band luminosity function (see Fig. A1). One at about K = 13.1 mag, the other at K = 13.7 mag. We interpret the former as the core helium burning objects. Note, that if we choose the second peak as the core helium burning objects, the determined distance to the cluster would increase by a factor of 1.3. The slope of the giant branch can be best fit using a metallicity of Z = 0.004. A lower metallicity results in a too steep slope of the RGB and a higher value in a too shallow slope. However, a range of Z = 0.001 to 0.008 can in principle explain the data. The RGB stars also form a compact group in the CCD, where the brighter stars show a smaller scatter in the colours than the fainter stars, in agreement with the photometric uncertainties.

We can fit an isochrone to the RGB in the CMD and CCD using the above mentioned metallicity, $\beta = 1.6$, a distance of 7 kpc, and an extinction of $A_K = 0.57$ mag. Since we do not detect any main sequence stars we cannot determine the age of the cluster. If we use our completeness limit as an indicator for how faint the main sequence stars need to be in order that we cannot detect them, the age of the cluster has to be at least 2 Gyr. Virtually no change in the quality of the fit is seen when using ages of 10 Gyr or above. The core helium burning objects allow to estimate the cluster distance within 500 pc. However, the upper limit for the age means that the cluster could be as close as 5 kpc (if the age is 12 Gyr). As for the other clusters the K-band extinction is uncertain by 0.05 mag.

The well populated giant branch, its low metallicity and the

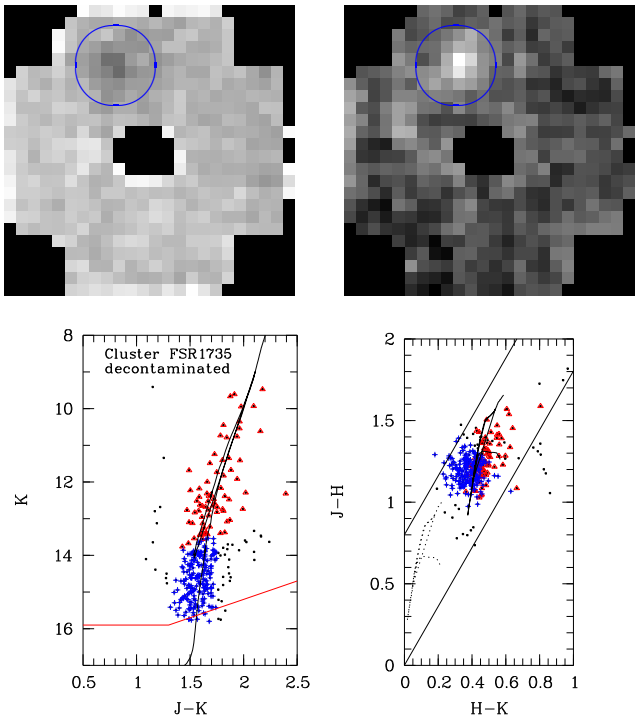

Figure 12. As Fig. 1 but for the cluster candidate FSR 1735. The plotted isochrone has log(age) = 9.9. See text for other parameters.

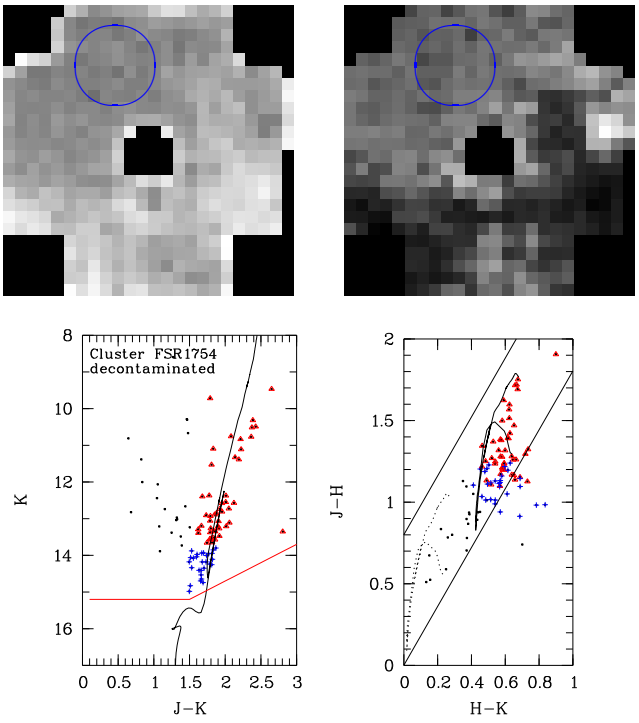

Figure 13. As Fig. 1 but for the cluster candidate FSR 1754. The plotted isochrone has log(age) = 9. See text for other parameters.

clusters position close to the Galactic Center, suggest that this object might indeed be much older. It could well be another (Palomar type?) globular cluster, similar to FSR 0190 (Froebrich et al. (2008)). The core radius of the object is determined to 0.9 pc using the RDP (Fig. B6).

We have remeasured the central coordinates of the cluster in our deeper images. The central coordinates are RA = 16:10:29.0, DEC = -53:44:48 (J2000), about one arcminute north-east of the values given in Froebrich et al. (2007b). There is an IRAS source (detected at 100 μm only) about 2.7' south of the cluster centre which seems, however, unrelated to the cluster.

3.12 FSR 1735

Here we re-analyse the data of FSR 1735, already presented as a globular cluster candidate in Froebrich et al. (2007a). This is to ensure a homogeneous analysis and interpretation of all the cluster candidates observed in this project. We re-analyse FSR 1735 using the entire field of observations, compared to just the small region around the cluster used in Froebrich et al. (2007a). The cluster image clearly shows a compact and populated cluster of stars. The SDM verifies this. In the REM we see that the colour of the stars in the cluster area is redder than in the field, most probably caused by the fact the we only see red giant cluster stars. This is very similar to the above discussed maps of FSR 1716. The south-eastern corner of the mosaic seems to possess a slightly smaller number of stars. We hence chose the western side of the image as the control field.

About 40 % to 45 % of the stars in the cluster area remain after the decontamination procedure. The decontaminated CMD of the cluster shows a well populated RGB/AGB (see Fig. 12). There is a peak in the K-band luminosity function at about K = 14 mag (see Fig. A2), which is interpreted as the core helium burning objects. The slope of the RGB is best fit using a metallicity of Z = 0.004, but as for FSR 1716 a range from Z = 0.001 to 0.008 can in principle explain the data. There are no main sequence stars detected, hence the age cannot be constrained. Using the detection limits of our photometry, we find that the age has to be larger than 2 Gyr. Indeed, we can increase this limit to an age above 8 Gyr, since such an age can better explain the CMD and CCD simultaneously. Slightly depending on the age, the distance to the cluster is 8.5 kpc and the reddening A_K = 0.7 mag. The used dust properties are β = 1.6. The uncertainty for the distance estimate is 500 pc, including the fact that we only have a lower limit for the age. The K-band extinction can be estimated within 0.05 mag. These results are in agreement with the parameters published for FSR 1735 in Froebrich et al. (2007a). The differences in the determined parameters are entirely due to the assumed age of 12 Gyr in the earlier publication. We have also remeasured the core radius of the cluster. Using the RDP (Fig. B7) it is determined as 0.95 pc, virtually identical to the value determined in Froebrich et al. (2007a).

3.13 FSR 1754

The image of this field shows no apparent overdensity of stars in the area of the cluster candidate. This is confirmed by the SDM, which is virtually flat in and around the object's position (see Fig. 13). The southern and western parts of the mosaic show a smaller number of stars. The REM indicates significant differences in the average colour of the stars in this area, caused by foreground clouds. We hence chose the eastern part of the image as the control area.

Only about 10 % of the stars remain after the decontamination. In the CMD they seem to show a populated giant branch (see Fig. 13). However, the slope would require metallicities in excess Z = 0.03 to fit. Furthermore, the positions of the stars in the

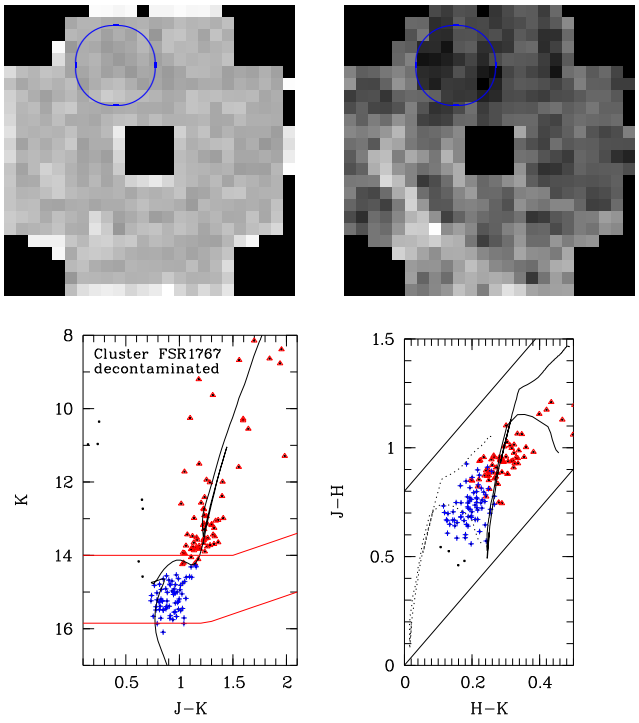

Figure 14. As Fig. 1 but for the cluster candidate FSR 1767. The plotted isochrone has log(age) = 9. See text for other parameters. The upper completeness limit in the CMD indicates the 2MASS limit. Clearly no isochrone can fit all the data.

CCD is not in agreement with the proposal of a giant branch. Especially the fainter stars are too close to the bottom of the reddening path. Furthermore, dust properties of $\beta < 1.4$ would be required to fit the stars with a single isochrone in CMD and CCD. The isochrone in Fig. 13 is plotted to clarify this argument and has the following parameters: Z = 0.03, β = 1.6, log(age) = 9, d = 10 kpc, and A_K = 0.8 mag. We conclude that FSR 1754 is not a cluster. This partly agrees with Bica et al. (2008), who classified this object as an uncertain candidate. The two main sequences in their analysis of 2MASS data are not evident in our analysis. In particular, the blue sequence disappears in our decontaminated CMD, most probably caused by a better choice of the control field (which is important given the large fluctuations visible in the SDM and REM - see Fig. 13).

3.14 FSR 1767

There is no apparent overdensity of stars in the image of the field around the cluster candidate. The SDM shows, however, a small increase in stellar numbers. In the REM we find that the cluster area suffers from less extinction than the south-eastern part of the mosaic. We have therefore chosen the western part of the image as control field.

The cluster was classified by Bonatto et al. (2007) as a globular cluster. With its parameters, [Fe/H] = -1.2 dex, A_V = 6.2mag and a distance of only 1.5 kpc it would be the 2^{nd} closest globular cluster after FSR 0584 (d = 1.4 kpc, Bica et al. (2007)), which is still under debate. The analysis of FSR 1767 in Bonatto et al.(2007) is based on 2MASS data (the upper detection limit in Fig. 14 and 15) and proper motions. Only a small number of cluster red giants has been found, and the upper end of the main sequence has been identified. With our much deeper images, we should be able to detect the main sequence stars down to lower masses and thus verify the claim of Bonatto et al. (2007) that this object is a globular cluster.

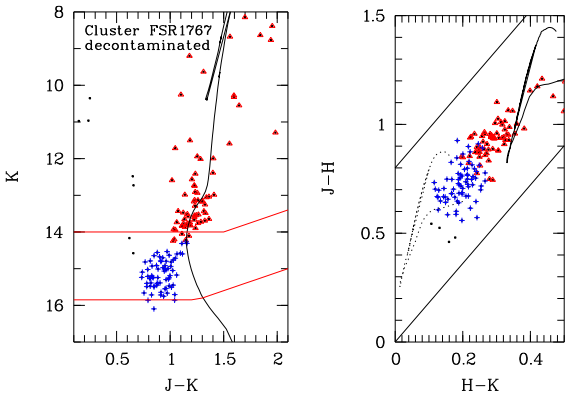

Figure 15. As bottom panel of Fig. 14 but using an isochrone with the cluster parameters for FSR 1767 as suggested by Bonatto et al. (2007); Age = 10 Gyr, Z = 0.001, d = 1.5kpc, A_K = 0.62 mag. Clearly this isochrone does not fit the data.

After decontamination only about 10 % of the stars remain in the cluster candidate area. The stars identified in Bonatto et al. (2007) as upper main sequence stars are also identifiable in the CMD from our data (see Fig. 14). However, overplotting an isochrone with the given cluster parameters (and assuming an age of about 10 Gyr) implies that the main sequence should continue towards fainter magnitudes and slightly redder colours (see Fig. 15). Nothing like this is identifiable in our data. There is a second group of stars above our detection limit (the lower line in Fig. 14) remaining in the CMD. We could interpret these as the top of the main sequence and the original group of stars as giants. A fit in the CMD (see Fig. 14) is then possible using an age of about 1 Gyr, a reddening of A_K = 0.5 mag and a distance of 6.5 kpc. However, in the CCD we clearly see that the two groups of stars cannot be fit by a single isochrone, since they possess different extinction values. We have to conclude that based on our deeper observations, FSR 1767 is not a globular cluster. It does not appear to be a stellar cluster at all, but rather a locally decreased amount of extinction mimicking a stellar overdensity.

4 DISCUSSION

4.1 Uncertainties

4.1.1 Photometry

The nature of our observations, stellar clusters in crowded fields, implies that the photometry suffers from relatively large errors. To ensure an as small as possible influence of these uncertainties, we used only the most reliable stellar magnitudes and colours for the analysis of the CMDs and CCDs. Only stars with quality flags from the Source Extractor software (Bertin & Arnouts (1996)) better than 3 are used (except for FSR 1735, were a flag better than 4 was chosen due to the very large crowding and hence small number of stars with a quality flag better than 3). Furthermore, the completeness limit in the cluster fields will be at brighter magnitudes than in the control fields. Thus, we only include stars in the analysis which are above the completeness limit in the cluster areas. This is also the limit indicated in all the CMDs.

Table 1. Measured properties of the clusters investigated in this paper. We list the FSR number, Right Ascension, Declination (J2000), determined age, K-band extinction A_K, distance d, metallicity Z, radius r, classification, and notes. Positions taken from: [1] Froebrich et al. (2007b); [2] Froebrich et al. (2007a); [3] Bonatto & Bica (2007b); [4] Kronberger et al. (2006); [5] measured in this paper. The classifications stand for: NC - not a cluster; OC - open cluster; YOC - young open cluster (age <100 Myr); GC - globular cluster; ? - classification uncertain; * If the clusters is very old (12 Gyr) the distance can be as small as 5 kpc; ** Metallicity is assumed to be solar; *** Uncertainty of the radii is 20 %; **** Radius could not be determined.

Name	α (2000)	δ (2000)	Age [Gyr]	A_K [mag]	d [kpc]	Z	r [pc]***	Class.	Notes
FSR 0002	17:32:32[1]	−27:03:51[1]	-	-	-	-	-	NC	
FSR 0023	17:57:35[1]	−22:52:32[1]	-	-	-	-	-	NC	
FSR 0088	18:50:38[1]	−04:11:17[1]	0.5±0.3	0.5±0.05	2.0±0.3	0.019**	****	OC	
FSR 0089	18:48:39[3]	−03:30:34[3]	1.0±0.3	1.0±0.05	2.2±0.3	0.019**	****	OC	confirms Bonatto & Bica (2007b)
FSR 0094	18:49:50[1]	−01:02:55[1]	-	-	-	-	-	NC	
FSR 1527	10:06:32[1]	−57:24:52[1]	-	-	-	-	-	NC	
FSR 1530	10:08:58.3[5]	−57:17:11[5]	$\leqslant$0.004	0.9±0.05	$2.5^{+0.5}_{-1.0}$	0.019**	0.15	YOC	
FSR 1570	11:08:40.6[4]	−60:42:50[4]	$0.008^{+0.008}_{-0.004}$	0.8±0.05	6.0±1.0	0.019**	0.35	YOC	confirms Pasquali et al. (2006)
FSR 1659	13:38:01[1]	−62:27:55[1]	-	-	-	-	-	NC	
FSR 1712	15:54:46.3[5]	−52:31:47[5]	$0.8^{+0.8}_{-0.4}$	1.4±0.1	1.8±0.3	0.019**	0.20	OC	
FSR 1716	16:10:29.0[5]	−53:44:48[5]	>2	0.57±0.05	7.0±0.5*	$0.004^{+0.004}_{-0.003}$	0.90	OC/GC?	
FSR 1735	16:52:10.6[2]	−47:03:29[2]	>8	0.7±0.05	8.5±0.5	$0.004^{+0.004}_{-0.003}$	0.95	GC?	confirms Froebrich et al. (2007a)
FSR 1754	17:15:01[1]	−39:06:07[1]	-	-	-	-	-	NC	partly confirms Bica et al. (2008)
FSR 1767	17:35:43[1]	−36:21:28[1]	-	-	-	-	-	NC	conflicts with Bonatto et al. (2007)

The observed scatter in the CMDs and also CCDs can thus be attributed to a number of causes. i) uncertainty in the photometry due to crowding; ii) scatter in the calibration due to the low spatial resolution of the 2MASS data; iii) small scale variable extinction towards the stars (A_V varies up to 0.5 mag from pixel to pixel in the fields close to some of the cluster candidates); iv) unresolved binaries; Given all those sources of error, the observed scatter in colour, for stars in a cluster with the same magnitude, of about 0.2 mag to 0.4 mag is understandable.

4.1.2 Cluster Parameters

In most cases the metallicity could not be determined. For all clusters with a fitted age below a few Gyr we assume a solar metallicity. We hence labeled the metallicities of these clusters with ** in Table 1. In the cases of the two old clusters, FSR 1716 and FSR 1735, the metallicities that fit the data range from Z = 0.001 to Z = 0.008 and the best fitting value of Z = 0.004 is listed in Table 1.

The determined values for extinction, distance and age are all dependent on each other in a systematic way. By changing one parameter slightly we will still be able to generate a good fit by adjusting the other two parameters. This is, however, only possible within a certain range, outside which it becomes impossible to fit CMDs and CCDs simultaneously. Typically the age of the clusters can be constrained by better than a factor of two, the K-band extinction to within 0.05 mag, and the distance within 20 %. Table 1 contains the uncertainties for the main parameters of the individual clusters.

The determined radii of the clusters vary dependent on which of the random realisation of the decontamination processes we use. Generally, for the cluster candidates with a high contrast between cluster area and field, the fitted radii vary by about 20 %. For the cases with a low contrast, inconclusive results are obtained, and the values in the Table 1 are marked by ****. The star density in the cluster centre is also highly uncertain, since it depends on: i) We only used stars with reliable photometry, hence we will miss more stars towards the cluster centre; ii) The completeness limit in the cluster centre differs from the control field, hence more stars are removed during the decontamination procedure. We hence refrain from listing the central star densities in Table 1.

4.2 General FSR cluster properties

A considerable number of clusters from the original FSR list have now been analysed in more detail by a variety of authors. Here we provide a brief summary of these investigations to date and a discussion of the properties of these new star clusters.

We have summarised the properly classified FSR clusters in Table D1. The table lists the FSR catalogue number and other identifications, Right Ascension and Declination (J2000), galactic coordinates, determined distance, K-band extinction, age, and metallicity. Furthermore we list the inferred position in the Galaxy, a classification, and the references where the values are taken from. Table E1 lists the FSR cluster candidates that have been investigated in detail but their nature could not be established, or they are classified as not being a stellar cluster. In these cases only the FSR number, other identifications, the coordinates, classification, and references are listed.

So far 74 FSR cluster candidates have been investigated in more detail. For 38 of these clusters parameters could be determined. Another 3 are embedded clusters with no parameters, 23 are not clusters, and 10 are uncertain cases. We cannot attempt to determine the contamination of the FSR sample from this statistics, since the investigated cluster candidates are not selected in an unbiased manner. There are, however, studies that have selected all FSR objects within certain areas (Koposov et al. (2008), Bonatto & Bica (2008), Bica et al. (2008)). These studies determine contamination rates between 40 and 60 %, in agreement with the original estimate of about 50 % in Froebrich et al. (2007b).

Out of the now classified FSR clusters, 8 are young open clusters with ages below 100 Myr (this includes the 3 embedded clusters with no determined parameters). A fraction of 50 % of the classified clusters have ages of more than 1 Gyr, and 20 % have ages above 2 Gyr. This has increased the sample of known old open clusters. In particular the FSR list revealed 7 old open clusters inside the solar circle, significantly enhancing the known number of these clusters.

In Figs. 16 and 17 we show the distribution of the classified FSR clusters in the Galaxy, and how they compare to the sample

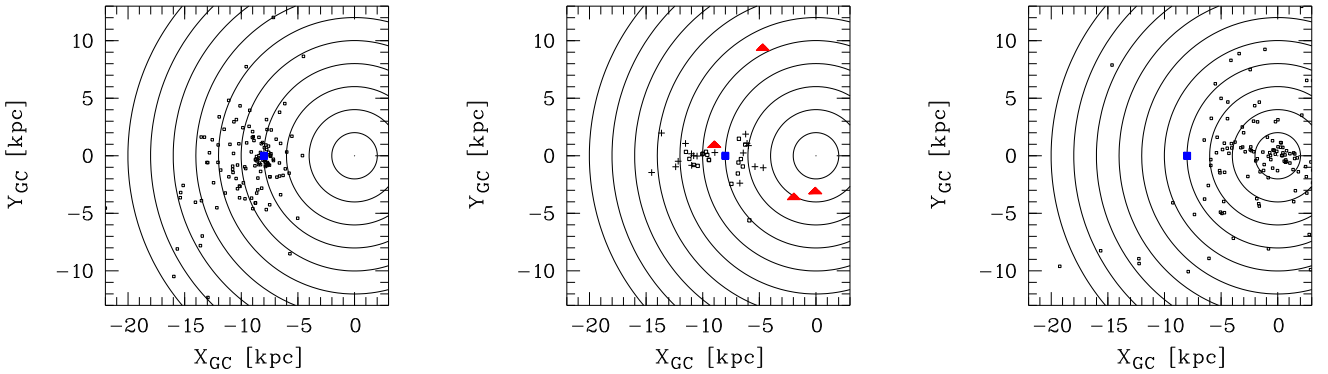

Figure 16. Distribution in the Galactic Plane of known old (age >1 Gyr) OCs (**left**), classified FSR clusters (**middle**), and known GCs (**right**). The blue square marks the position of the Sun. The red triangles in the middle panel represent the FSR GC candidates, crosses the old (age $\geqslant 1$ Gyr), and squares the young (age <1 Gyr) OCs in the FSR sample. We assumed a galactocentric distance of the Sun of 8 kpc.

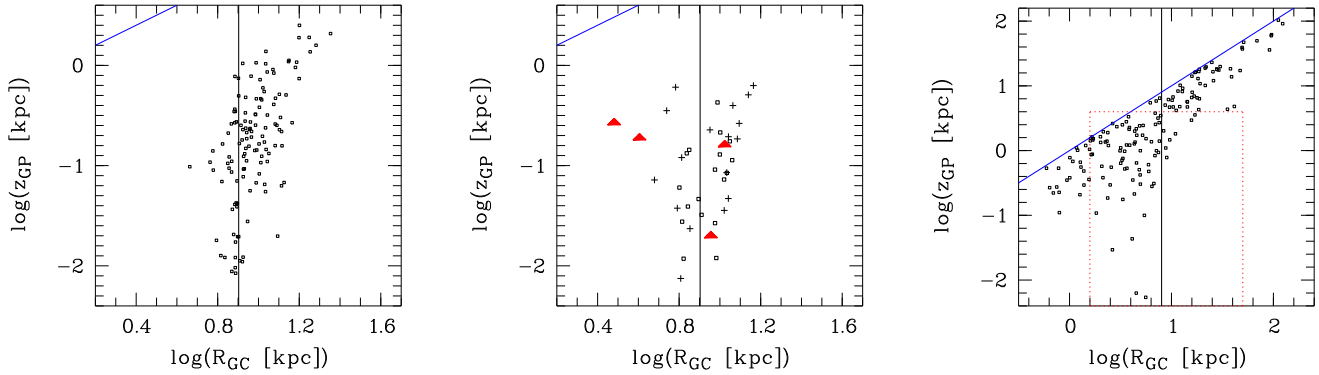

Figure 17. Distance to the Galactic Centre ($R_{\rm GC}$) vs. height above the Galactic Plane ($z_{\rm GP}$) of known old (age >1 Gyr) OCs (**left**), classified FSR clusters (**middle**), and known GCs (**right**). The black vertical line marks the position of the Sun, the blue diagonal line represents the maximum height above the plane for a given distance from the centre. The red triangles in the middle panel represent the FSR GC candidates, crosses the old (age $\geqslant 1$ Gyr), and squares the young (age <1 Gyr) OCs in the FSR sample. We assumed a galactocentric distance of the Sun of 8 kpc. The dotted box in the right panel marks the region shown in the left and middle panel.

of known old (age $\geqslant 1$ Gyr) open clusters (taken from WEBDA[3]) and known globular clusters (taken from Harris (1996)). We plot young and old open clusters and globular cluster candidates among the FSR objects using different symbols. Despite the unknown selection effects in the sample of properly classified FSR clusters, a number of trends are evident: i) There is a large fraction of old open clusters in the sample. This includes old clusters inside and outside the solar circle and with distances of more than 1 kpc from the Sun. The complete FSR list will significantly increase the number of known old open clusters. ii) Two of the globular cluster candidates (FSR 1716, 1735) nicely follow the distribution of the known globular clusters in the Milky Way. iii) The 10 ± 3 'missing' globulars near the Galactic Centre (Ivanov et al. (2005)) are not contained in the FSR list. These clusters are either really not there, hidden behind very dense clouds, or intrinsically faint. Given the fact that we detected FSR 1735, the number of intrinsically bright globular clusters near the Galactic Centre that have been missed by the FSR survey is very small.

[3] `http://www.univie.ac.at/webda/`

5 CONCLUSIONS

We have properly (re)-classified 14 star cluster candidates from the list of Froebrich et al. (2007b). We utilised new deep NIR photometry obtained at the NTT. Star density maps, extinction maps, colour-magnitude diagrams, and colour-colour diagrams, facilitated by radial star density profiles and luminosity functions were used for the analysis of the individual objects. Seven FSR cluster candidates are found to be real stellar clusters, seven candidates are only star density enhancements.

Out of the seven classified star clusters, we have identified two young clusters with massive stars (FSR 1530, FSR 1570 - investigated also by Pasquali et al. (2006)); three intermediate aged open clusters (FSR 0088, FSR 0089 - confirms Bonatto & Bica (2007b), FSR 1712); and two globular cluster candidates (FSR 1716, FSR 1735 confirms Froebrich et al. (2007a)) with well populated giant branches.

We show that 2MASS data alone can sometimes be misleading or insufficient when classifying (globular) cluster candidates. Our analysis of deep high spatial resolution photometry is superior in some cases, especially for cluster candidates in crowded fields near the Galactic Plane. One particular example is the cluster candidate FSR 1767. It has been classified as a globular cluster by Bonatto et al. (2007). Our new data shows that their interpretation of the insufficient 2MASS data is incorrect, and we conclude that FSR 1767 is

not a globular cluster. Most probably this object is just an apparent stellar overdensity caused by a locally decreased amount of extinction, mimicking a stellar cluster.

So far a total of 74 cluster candidates from the FSR list (containing 1021 candidate clusters) has been analysed in detail. The statistics points to a contamination of the FSR sample with stellar overdensities of 40 % to 60 %, in agreement with the original estimate of Froebrich et al. (2007b). A large fraction of the so far investigated FSR clusters have turned out to be old stellar clusters with ages above 1 Gyr. This significantly increases the number of known old clusters, in particular inside the solar circle. Mining the FSR catalogue for such type of clusters has the potential to provide new insights into long-term cluster evolution and the associated physical processes.

ACKNOWLEDGMENTS

This publication makes use of data products from the Two Micron All Sky Survey, which is a joint project of the University of Massachusetts and the Infrared Processing and Analysis Center/California Institute of Technology, funded by the National Aeronautics and Space Administration and the National Science Foundation. This research has made use of the SIMBAD database, operated at CDS, Strasbourg, France. This research has made use of the WEBDA database, operated at the Institute for Astronomy of the University of Vienna. These observations have been funded by the Optical Infrared Coordination network (OPTICON), a major international collaboration supported by the Research Infrastructures Programme of the European Commission's Sixth Framework Programme.

REFERENCES

Bertin, E., Arnouts, S. 1996, A&AS, 117, 393
Beuther, H., Churchwell, E.B., McKee, C.F., Tan, J.C. 2007, in Protostars and Planets V, B. Reipurth, D. Jewitt, and K. Keil (eds.), University of Arizona Press, Tucson, 951, 165
Bica, E., Bonatto, C., 2008, MNRAS, 384, 1733
Bica, E., Bonatto, C., Camargo, D. 2008, MNRAS, 384, 349
Bica, E., Bonatto, C., Barbuy, B., Ortolani, S. 2006, A&A, 450, 105
Bica, E., Bonatto, C., Dutra, C.M. 2008, A&A, in press
Bica, E., Bonatto, C., Ortolani, S., Barbuy, B. 2007, A&A, 472, 483
Bonatto, C., Bica, E. 2007, MNRAS, 377, 1301
Bonatto, C., Bica, E. 2007, A&A, 473, 445
Bonatto, C., Bica, E. 2008, A&A, 485, 81
Bonatto, C., Bica, E., Ortolani, S., Barbuy, B. 2007, MNRAS, 381, 45
Bonnell, I.A., Larson, R.B., Zinnecker, H. 2007, in Protostars and Planets V, B. Reipurth, D. Jewitt, and K. Keil (eds.), University of Arizona Press, Tucson, 951, 149
Brodie, J.P., Larsen, S.S. 2002, AJ, 124, 1410
Cavanagh, B., Hirst, P., Jenness, T., Economou, F., Currie, M.J., Todd, S., Ryder, S.D. 2003, in Astronomical Data Analysis Software and Systems XII ASP Conference Series, H.E. Payne, R.I. Jedrzejewski, and R.N. Hook, eds., 295, 237
Davies, M.B., Piotto, G., de Angeli, F., 2004, MNRAS, 349, 129
Dutra, C.M., Santiago, B.X., Bica, E. 2002, A&A, 381, 219
Froebrich, D., Meusinger, H., Scholz, A. 2007, MNRAS, 377, 54L
Froebrich, D., Murphy, G.C., Smith, M.D., Walsh, J., Del Burgo, C., 2007, MNRAS, 378, 1447
Froebrich, D., Scholz, A., Raftery, C.L. 2007, MNRAS, 374, 399
Froebrich, D., Meusinger, H., Davis, C.J. 2008, MNRAS, 383, 45
Froebrich, D. & del Burgo, C. 2006, MNRAS, 369, 1901
Girardi, L., Bertelli, G., Bressan, A., et al. 2002, A&A, 391, 195
Harris, W.E. 1996, AJ, 112, 1487
Huxor, A.P., Tanvir, N.R., Irwin, M.J., et al. 2005, MNRAS, 360, 1007
Ivanov, V.D., Kurtev, R., Borissova, J. 2005, A&A, 442, 195
Koposov, S.E., Glushkova, E.V., Zolotukhin, I.Y., 2008, A&A, 486, 771
Kronberger, M., Teutsch, P., Alessi, B., et al. 2006, A&A, 447, 921
Leitherer, C., Schaerer, D., Goldader, J.D., et al. 1999, ApJS, 123, 3
Martini, P., Ho, L.C. 2004, ApJ, 610, 233
Mathis, J.S. 1990, ARA&A, 28, 37
Mieske, S., Hilker, M., Infante, L. 2002, A&A, 383, 823
Mieske, S., Hilker, M., Infante, L. 2004, A&A, 418, 445
Pasquali, A., Comerón, F., Nota, A. 2006, A&A, 448, 589
Robin, A.C., Reylé, C., Derrière, S., Picaud, S. 2003, A&A, 409, 523
Roche, P.F., Lucas, P.W., Mackay, C.D., et al. 2003, in Instrument Design and Performance for Optical/Infrared Ground-based Telescopes. Edited by Iye, Masanori; Moorwood, Alan F. M. Proceedings of the SPIE, 4841, 901
Salaris, M., Girardi, L. 2002, MNRAS, 337, 332
Skrutskie, M.F., Cutri, R.M., Stiening, R., et al. 2006, AJ, 131, 1163
Weidner, C., Kroupa, P. 2006, MNRAS, 365, 1333
West, M.J., Côte, P., Marzke, R.O., Jordan, A. 2004, Nature, 427, 31

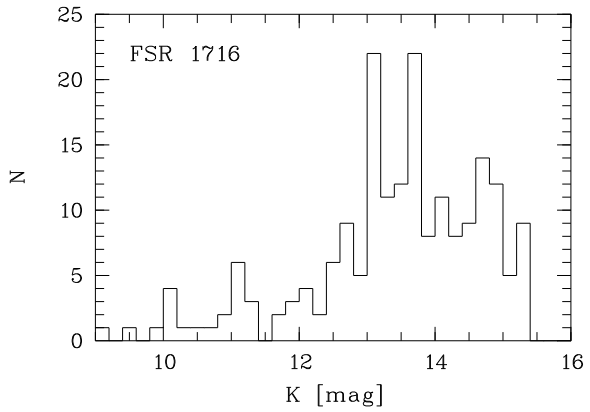

Figure A1. One realisation of the K-band luminosity function of the decontaminated cluster area of FSR 1716.

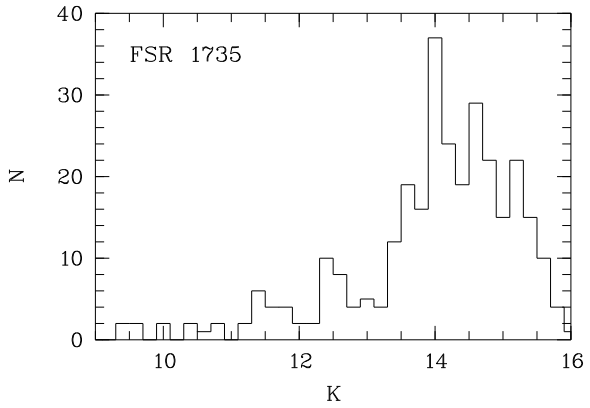

Figure A2. K-band luminosity function of the decontaminated cluster area of FSR 1735.

APPENDIX A: K-BAND LUMINOSITY FUNCTIONS

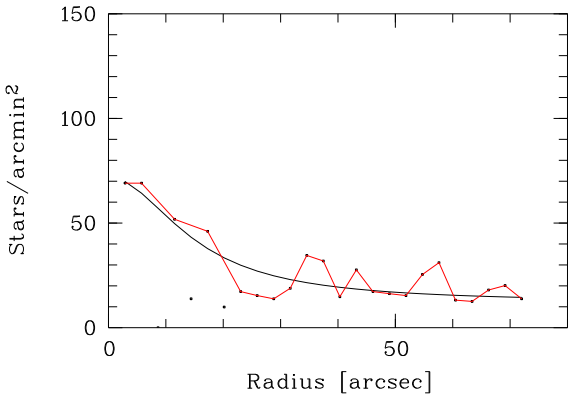

Figure B1. One realisation of the K-band RDP (dots, red line) of the decontaminated region of FSR 0088. The solid black line represents the best fit using a core radius of 15”. The dots are RDP points more than 2σ away from the general profile, and are hence not used in the fit.

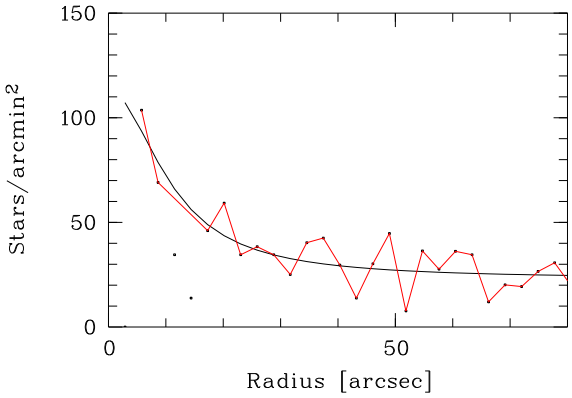

Figure B2. As Fig. B1 but for FSR 0089. The solid black line represents the best fit using a core radius of 11”.

APPENDIX B: K-BAND RADIAL STAR DENSITY PROFILES

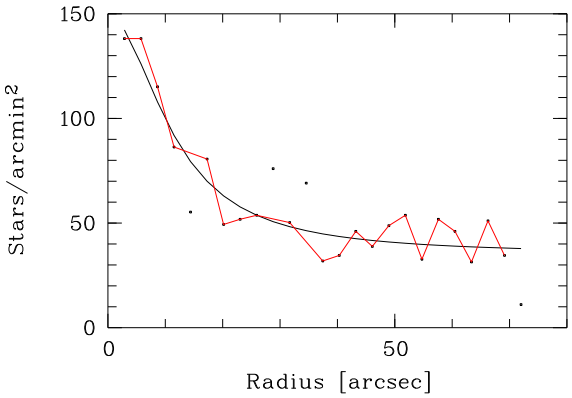

Figure B3. As Fig. B1 but for FSR 1530. The solid black line represents the best fit using a core radius of 11.5”.

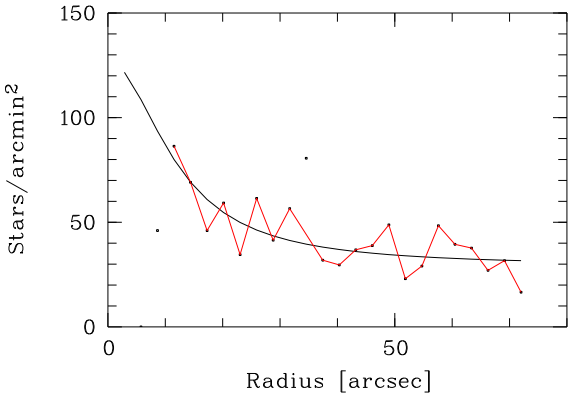

Figure B4. As Fig. B1 but for FSR 1570. The solid black line represents the best fit using a core radius of 12”.

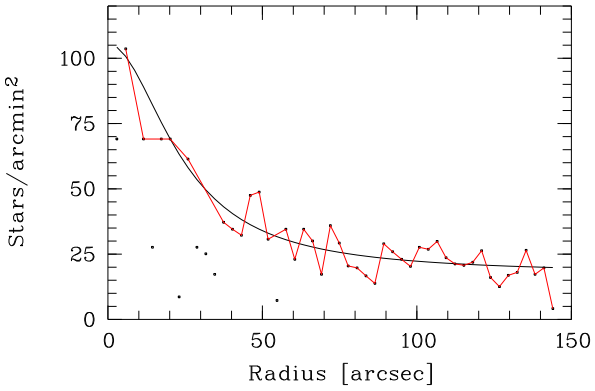

Figure B5. As Fig. B1 but for FSR 1712. The solid black line represents the best fit using a core radius of 24”.

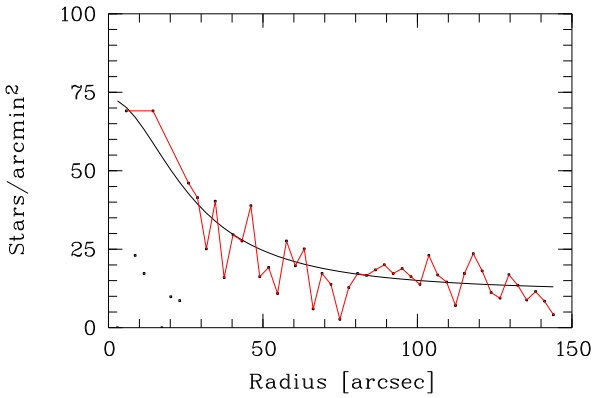

Figure B6. As Fig. B1 but for FSR 1716. The solid black line represents the best fit using a core radius of 26.5”.

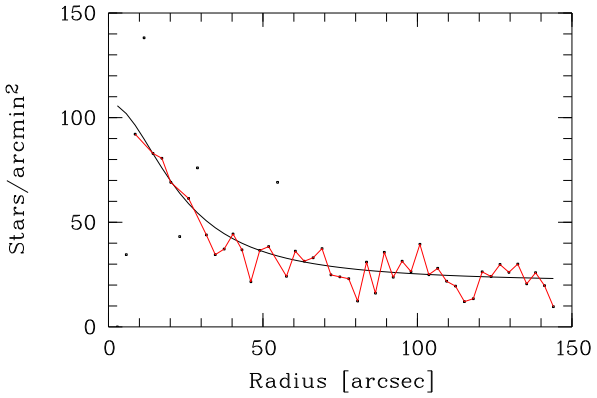

Figure B7. As Fig. B1 but for FSR 1735. The solid black line represents the best fit using a core radius of 23”.

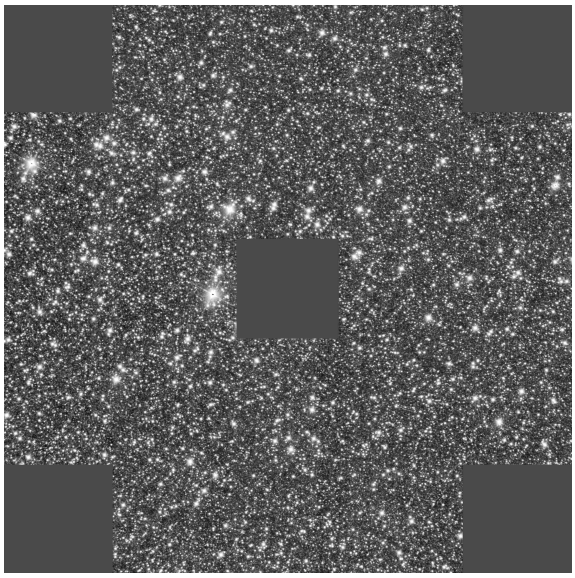

Figure C1. Grey scale representation of the K-band mosaic of cluster candidate FSR 0002. The image size is about 11.7' x 11.7', north is up and east to the left. The cluster candidate is positioned in the upper left part of the mosaic.

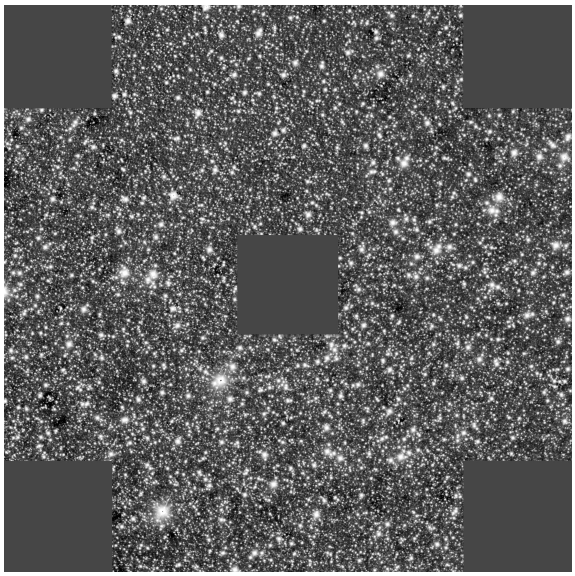

Figure C2. As Fig. C1 but for the cluster candidate FSR 0023.

APPENDIX C: K-BAND IMAGES OF THE CLUSTER CANDIDATES

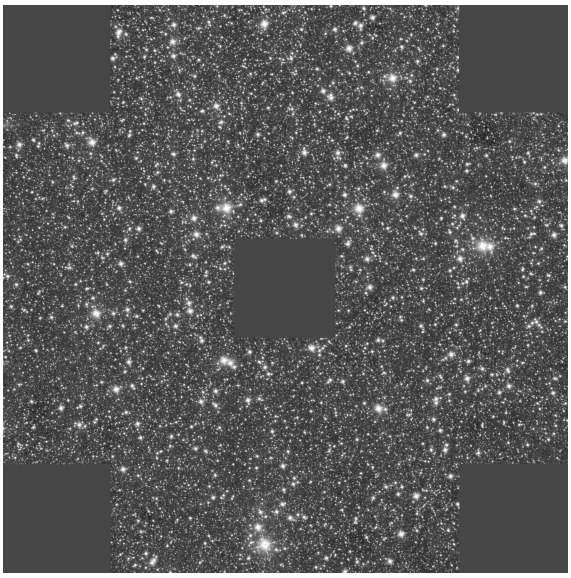

Figure C3. As Fig. C1 but for the cluster candidate FSR 0088.

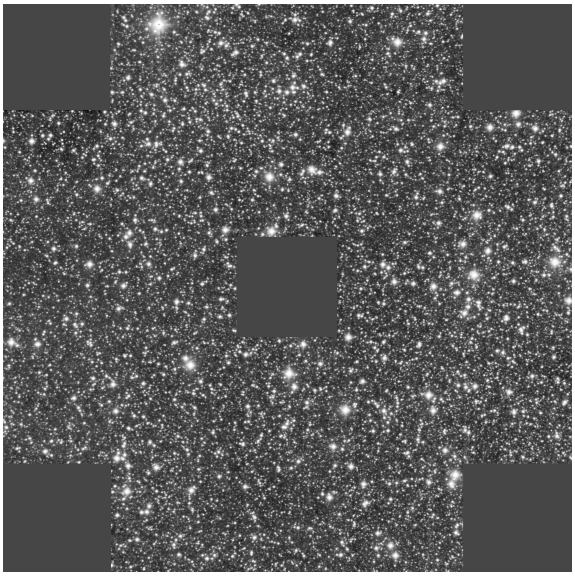

Figure C4. As Fig. C1 but for the cluster candidate FSR 0089.

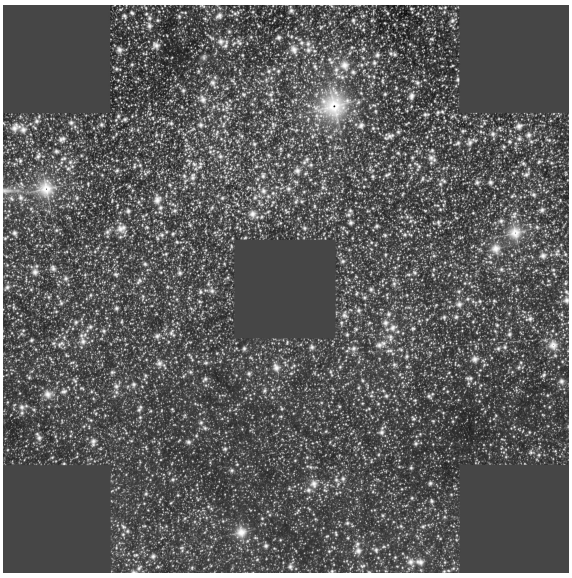

Figure C5. As Fig. C1 but for the cluster candidate FSR 0094.

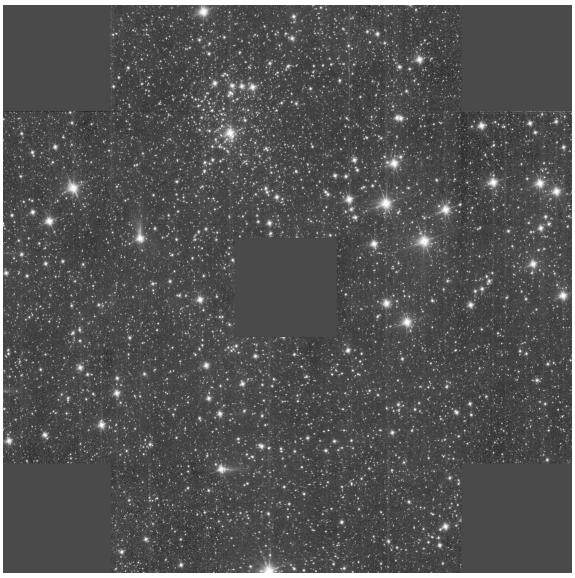

Figure C7. As Fig. C1 but for the cluster candidate FSR 1530.

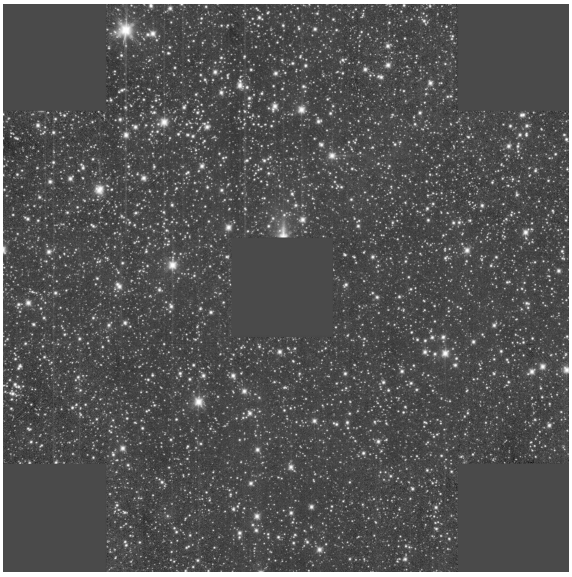

Figure C6. As Fig. C1 but for the cluster candidate FSR 1527.

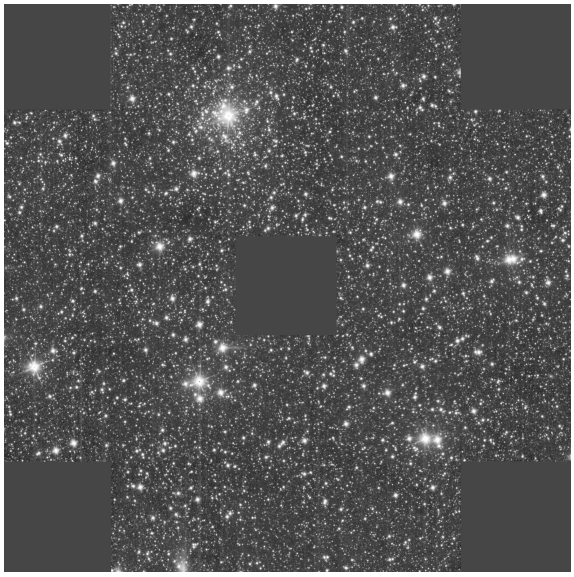

Figure C8. As Fig. C1 but for the cluster candidate FSR 1570.

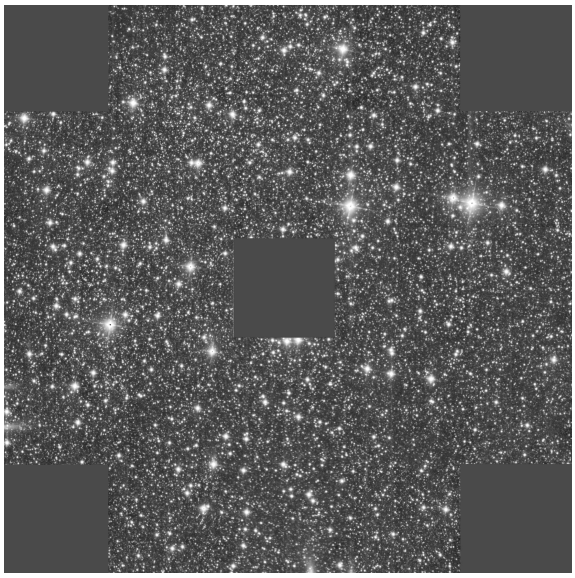

Figure C9. As Fig. C1 but for the cluster candidate FSR 1659.

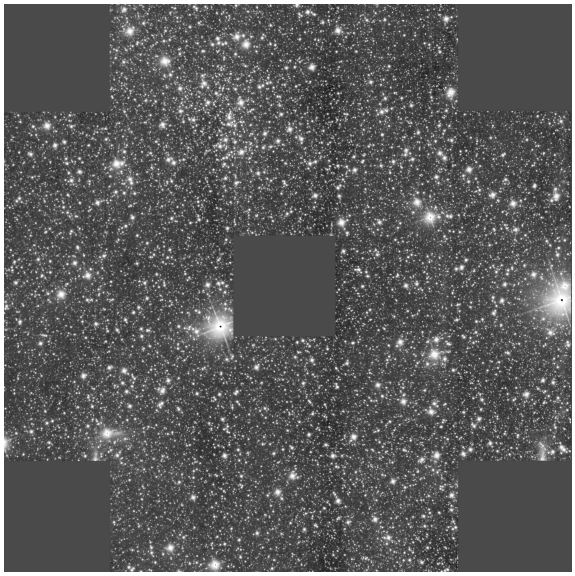

Figure C10. As Fig. C1 but for the cluster candidate FSR 1712.

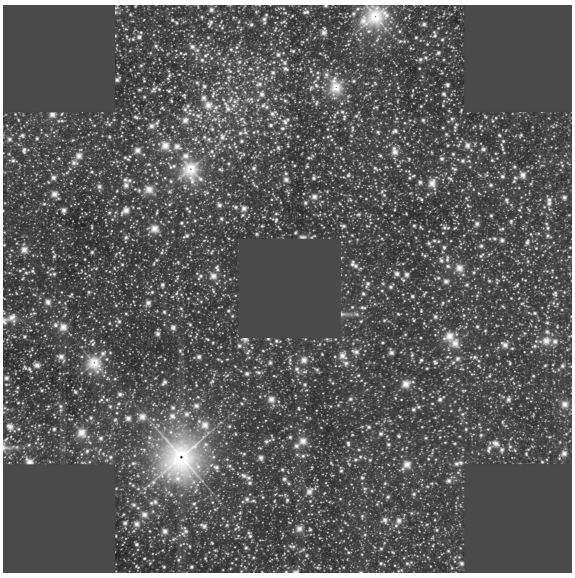

Figure C11. As Fig. C1 but for the cluster candidate FSR 1716.

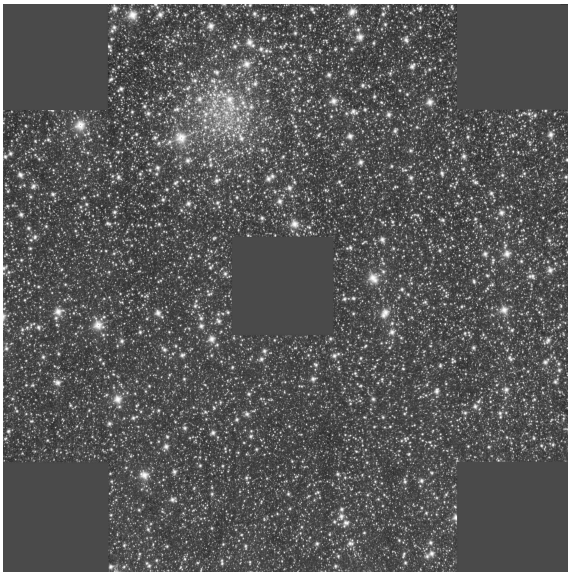

Figure C12. As Fig. C1 but for the cluster candidate FSR 1735.

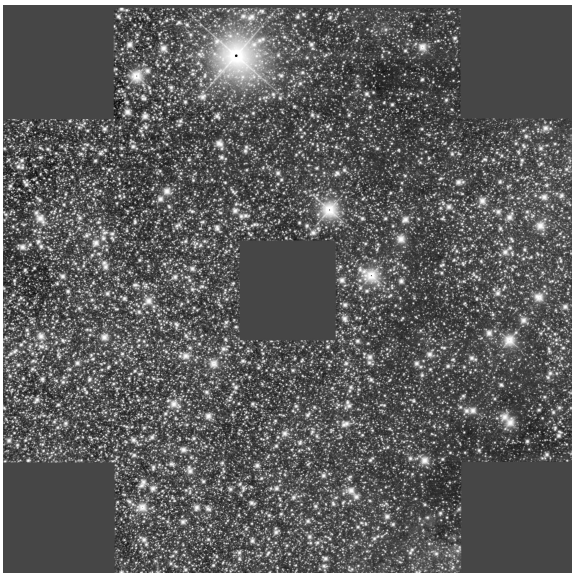

Figure C13. As Fig. C1 but for the cluster candidate FSR 1754.

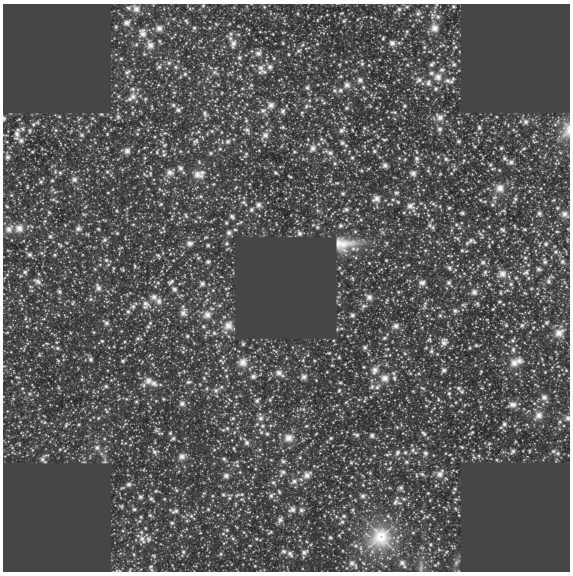

Figure C14. As Fig. C1 but for the cluster candidate FSR 1767.

APPENDIX D: PARAMETERS OF PROPERLY CLASSIFIED FSR CLUSTERS

APPENDIX E: LIST OF OTHER INVESTIGATED FSR CANDIDATES

Table D1. Summary of the properties of all FSR clusters analysed in detail so far and that are clearly star clusters. The table lists: FSR number and other identifications, Right Ascension, Declination (J2000), Galactic Coordinates (l,b), Distance d, Extinction A_K, Age, Metallicity Z, Galactocentric Distance $R_{\rm GC}$, Distance above the Galactic Plane $z_{\rm GP}$, Classification, and References. The classifications stand for: OC - open cluster; YOC - young open cluster (age <100 Myr); GC - globular cluster; ? - classification, or parameter uncertain. We assumed a galactocentric distance of the Sun of 8 kpc.

Name(s)	α (2000)	δ (2000)	l [deg]	b [deg]	d [kpc]	A_K [mag]	Age [Gyr]	Z	$R_{\rm GC}$ [kpc]	$z_{\rm GP}$ [pc]	Class.	Reference
FSR 0031	18:06:29.0	−21:22:33	8.9062	−0.2680	1.6	0.5	1.1	0.019?	6.4	-7.5	OC	Bonatto & Bica (2007b)
FSR 0070	19:30:02.0	−15:10:01	23.4404	−15.2646	2.3	0.1	5.0	0.019?	6.1	-610	OC	Bica et al. (2008)
FSR 0088	18:50:38.0	−04:11:17	29.1119	−1.7298	2.0	0.5	0.5	0.019?	6.3	-60	OC	this paper
FSR 0089	18:48:39.0	−03:30:34	29.4908	−0.9803	2.2	1.0	1.0	0.019?	6.2	-38	OC	Bonatto & Bica (2007b) this paper
FSR 0124	19:06:52.0	+13:15:21	46.4754	+2.6526	2.6	0.4	1.0	0.019?	6.5	120	OC	Bica et al. (2008)
FSR 0133	19:29:48.5	+15:33:36	51.1120	−1.1780	1.9	0.7	0.6	0.019?	7.0	-39	OC	Bica et al. (2008)
FSR 0190	20:05:31.3	+33:34:09	70.7303	+0.9498	10.0	0.8	>7	0.002	10.5	170	OC/GC?	Froebrich et al. (2008)
FSR 0584	02:27:15.0	+61:37:28	134.0579	+0.8399	1.4	1.0	10.0?	0.0002?	9.0	21	GC?	Bica et al. (2007)
FSR 0705	05:11:43.0	+47:41:42	160.7071	+4.8607	6.0	0.1	1.5	0.019?	13.8	510	OC	Bonatto & Bica (2008)
NGC 1798												
FSR 0729	05:25:55.0	+46:29:46	163.0794	+6.1646	3.7	0.05	1.0	0.019?	11.6	400	OC	Bonatto & Bica (2008)
NGC 1883												
FSR 0730	06:02:34.6	+49:51:36	163.2463	+13.1319	1.0	0.05	1.2	0.019?	8.9	230	OC	Bonatto & Bica (2008)
NGC 2126												
Melotte 39												
Collinder 78												
FSR 0756	04:24:13.4	+29:42:14	168.6494	−13.7190	1.8	0.3	0.3	0.019?	9.7	-430	OC	Bonatto & Bica (2008)
FSR 0793	05:24:21.6	+32:36:03	174.4474	−1.8561	3.5	0.15	0.9	0.019?	11.5	-110	OC	Bonatto & Bica (2008)
Berkeley 69												
FSR 0795	05:47:28.6	+35:25:56	174.6448	+3.7033	2.0	0.35	<0.4	0.019?	10.0	130	OC	Koposov et al. (2008)
Koposov 10												
FSR 0802	06:00:56.2	+35:16:36	176.1598	+6.0004	2.05	0.13	0.8	0.019?	10.0	210	OC	Koposov et al. (2008)
Koposov 12												
FSR 0810	05:40:57.0	+32:16:16	176.6344	+0.8968	3.0	0.25	1.0	0.019?	11.0	47	OC	Bonatto & Bica (2008)
Berkeley 71												
FSR 0814	05:36:46.1	+31:11:46	177.0691	−0.4288	1.6	0.3	<0.22	0.019?	9.6	-12	YOC	Bonatto & Bica (2008)
Koposov 36												Koposov et al. (2008)
FSR 0828	05:52:14.6	+29:55:09	179.9001	+1.7425	2.8	0.17	2.0	0.019?	10.9	85	OC	Koposov et al. (2008)
Koposov 43												
FSR 0834	05:50:07.0	+28:53:28	180.5474	+0.8191	2.5	0.0	4.5	0.019?	10.5	36	OC	Bonatto & Bica (2008)
Czernik 23												
FSR 0856	06:08:56.2	+26:15:49	184.9029	+3.1308	3.2	0.15	<0.32	0.019?	11.2	170	OC	Koposov et al. (2008)
Koposov 53												
FSR 0869	06:10:01.9	+24:32:55	186.5267	+2.5208	4.2	0.15	1.4	0.019?	12.2	180	OC	Bonatto & Bica (2008)
Koposov 63												Koposov et al. (2008)
FSR 0911	06:25:01.0	+19:50:55	192.3100	+3.3600	4.5	0.16	7.0	0.019?	12.4	-580	OC	Bonatto & Bica (2008)
Cl 1 in Bochum 1												Bica et al. (2008)
FSR 0917	06:33:16.2	+20:31:08	192.6094	+5.3837	6.7	0.03	1.2	0.019?	14.6	630	OC	Bonatto & Bica (2008)
Berkeley 23												
FSR 0923	06:10:36.0	+16:58:16	193.2296	−1.0187	1.5	0.45	0.5	0.019?	9.5	-27	OC	Bonatto & Bica (2008)
FSR 0932	06:04:26.4	+14:33:20	194.6240	−3.4866	1.5	0.3	0.15	0.019?	9.5	-91	OC	Bonatto & Bica (2008)
FSR 0942	06:05:58.0	+13:40:06	195.5810	−3.5950	3.1	0.2	1.0	0.019?	11.0	-190	OC	Bonatto & Bica (2008)
FSR 0948	06:25:52.8	+15:50:15	195.9645	+1.6710	2.9	0.15	0.03	0.019?	10.8	85	YOC	Bonatto & Bica (2008)
FSR 0974	06:32:41.3	+12:31:55	199.6598	+1.6015	2.6	0.2	0.4	0.019?	10.5	73	OC	Bonatto & Bica (2008)
FSR 1530	10:08:58.3	−57:17:11	282.3294	−1.0628	2.5	0.9	$\leqslant$0.004	0.019?	7.9	-46	YOC	this paper
FSR 1570	11:08:40.6	−60:42:50	290.6888	−0.3083	6.0	0.8	0.008	0.019?	8.1	-32	YOC	Pasquali et al. (2006) this paper
FSR 1603	12:09:45.0	−62:59:17	298.2191	−0.4984	2.7	0.2	1.0	0.019?	7.1	-23	OC	Bica & Bonatto (2008)
FSR 1644	13:18:02.9	−67:04:34	305.5257	−4.3385	1.9	0.1	0.6	0.019?	7.1	-140	OC	Bica et al. (2008)
Harvard 8												
Cr 268												
FSR 1712	15:54:46.3	−52:31:47	328.8084	+0.8786	1.8	1.4	0.8	0.019?	6.5	28	OC	this paper
FSR 1716	16:10:29.0	−53:44:48	329.7779	−1.5893	7.0	0.57	>2	0.004	4.0	-190	OC/GC?	this paper
FSR 1723	15:55:05.0	−46:00:51	333.0269	+5.8517	1.3	0.01	0.8	0.019?	6.9	130	OC	Bica et al. (2008)
ESO 275SC1												
FSR 1735	16:52:10.6	−47:03:29	339.1877	−1.8533	8.5	0.7	>8	0.004	3.0	-270	GC?	Froebrich et al. (2007a) this paper
FSR 1737	16:18:21.0	−40:14:35	340.0953	+7.2499	2.8	0.2	>5	0.019?	5.5	350	OC	Bica et al. (2008)
FSR 1744	16:51:36.0	−42:24:55	342.7060	+1.1783	3.5	0.85	1.0	0.019?	4.8	72	OC	Bonatto & Bica (2007b)
FSR 1755	17:12:20.0	−38:27:44	348.2458	+0.4825	1.4	0.45	<0.005	0.019?	6.6	12	YOC	Bica & Bonatto (2008)

Table E1. Summary of the properties of all FSR clusters analysed in detail so far and were the classification is unclear, no parameters are derived or which are clearly not star clusters. The table lists: FSR number and other identifications, Right Ascension, Declination (J2000), Galactic Coordinates (l,b), Classification, and References. The classifications stand for: NC - not a cluster; OC - open cluster; EC - embedded cluster; ? - classification uncertain.

Name	α (2000)	δ (2000)	l [deg]	b [deg]	Class.	Reference
FSR 0002	17:32:32.0	−27:03:51	0.0462	+3.4416	NC	this paper
FSR 0010	16:40:49.0	−16:01:09	2.1485	+19.6176	OC?	Bica et al. (2008)
FSR 0023	17:57:35.0	−22:52:32	6.5839	+0.7827	NC	this paper
FSR 0041	17:03:30.0	−08:51:13	11.7384	+19.1982	NC	Bica et al. (2008)
FSR 0091	17:38:21.0	+05:43:14	29.6887	+18.8502	NC	Bica et al. (2008)
FSR 0094	18:49:50.0	−01:02:55	31.8158	−0.1213	NC	this paper
FSR 0098	18:47:36.0	+00:35:46	33.0251	+1.1256	OC?	Bica et al. (2008)
FSR 0114	20:09:09.0	−02:13:03	40.0167	−18.2675	NC	Bica et al. (2008)
FSR 0119	18:23:05.0	+15:49:12	44.0994	+13.2956	NC	Bica et al. (2008)
FSR 0128	20:31:10.1	+04:45:07	49.2922	−19.6403	NC	Bica et al. (2008)
FSR 0744	04:59:30.0	+38:00:42	167.0846	−2.7641	NC	Bonatto & Bica (2008)
FSR 0773	04:29:37.0	+26:00:14	172.3124	−15.3117	?	Bonatto & Bica (2008)
FSR 0776	06:07:24.0	+39:49:34	172.7400	+9.2946	NC	Bonatto & Bica (2008)
FSR 0784	05:40:44.1	+35:55:25	173.5096	+2.7915	EC	Koposov et al. (2008)
Koposov 7						
FSR 0801	04:47:04.8	+24:54:00	175.7930	−12.9947	NC	Bonatto & Bica (2008)
FSR 0839	06:03:58.0	+30:15:41	180.8678	+4.1118	EC	Koposov et al. (2008)
Koposov 41						
FSR 0841	05:06:13.4	+21:33:27	181.2319	−11.4928	NC	Bonatto & Bica (2008)
FSR 0849	05:51:11.0	+25:46:41	183.3426	−0.5718	EC	Koposov et al. (2008)
Koposov 58						
FSR 0851	05:14:44.9	+19:47:31	183.8703	−10.8657	?	Bonatto & Bica (2008)
FSR 0855	05:42:21.6	+22:49:48	184.8249	−3.8180	?	Bonatto & Bica (2008)
FSR 0882	05:27:51.1	+16:53:49	188.0656	−9.8578	?	Bonatto & Bica (2008)
FSR 0884	05:32:21.0	+17:11:02	188.4011	−8.7954	?	Bonatto & Bica (2008)
FSR 0894	06:04:05.0	+20:16:51	189.5866	−0.7570	NC	Bonatto & Bica (2008)
FSR 0927	06:24:10.0	+18:01:30	193.8370	+2.3286	NC	Bonatto & Bica (2008)
FSR 0956	06:12:25.0	+13:00:26	196.9185	−2.5390	NC	Bonatto & Bica (2008)
FSR 1527	10:06:32.0	−57:24:52	282.1369	−1.3586	NC	this paper
FSR 1635	12:54:57.0	−43:29:24	303.6073	+19.3771	NC	Bica et al. (2008)
FSR 1647	13:45:48.0	−73:57:29	306.7313	−11.4887	NC	Bica et al. (2008)
FSR 1659	13:38:01.0	−62:27:55	308.2860	−0.0787	NC	this paper
FSR 1685	14:57:14.9	−64:57:22	315.7477	−5.2629	NC	Bica et al. (2008)
FSR 1695	14:33:38.0	−49:10:09	319.5904	+10.3687	NC	Bica et al. (2008)
FSR 1740	17:49:17.8	−51:31:55	340.7279	−12.0481	OC?	Bica et al. (2008)
FSR 1754	17:15:03.4	−39:05:46	348.0432	−0.3191	NC	Bica et al. (2008)
						this paper
FSR 1767	17:35:43.0	−36:21:28	352.6010	−2.1662	NC	Bonatto et al. (2007)
						this paper
FSR 1769	17:04:41.3	−31:00:43	353.3068	+6.1797	OC?	Bica et al. (2008)